ANALYSIS OF WATERSHED PARAMETERS CONTROLLING TURBIDITY FOLLOWING THE WEST FORK COMPLEX FIRE

by

Nicholas Hall

A thesis submitted to the Faculty and the Board of Trustees of the Colorado School of Mines in partial fulfillment of the requirements for the degree of Master of Science (Hydrology).

Golden, Colorado

Date _____

Signed: _____

Nicholas Hall

Signed: _____

Dr. Kamini Singha
Thesis Advisor

Golden, Colorado

Date _____

Signed: _____

Dr. Josh Sharp
Associate Professor and Director
Hydrologic Science and Engineering Program

ABSTRACT

In this thesis, I explore watershed characteristics associated with increased turbidity following wildfires, with the goal of developing relations between turbidity and slope aspect, soil type, slope, and vegetation health from the 2013 West Fork Complex Fire (WFC) in southwest Colorado, USA. Turbidity, precipitation, and stream discharge were previously measured from May to September in 2015 and 2016 in seven watersheds, four burned and three unburned. I then characterized slope, slope aspect, soil type, vegetation, precipitation, and burn severity for each of the seven watersheds, as well as inside the burned areas of the four burned watersheds. I used turbidity as a proxy for sedimentation in each watershed as the dependent variable.

Results indicate that from July to September of both 2015 and 2016, burned watersheds had larger spikes in turbidity following precipitation events than unburned watersheds. Higher burn severity and poor vegetation recovery were associated with the strongest positive correlations between total storm volume and turbidity responses. Enhanced Vegetation Index (EVI) was not consistently able to predict which watersheds would experience elevated turbidity following precipitation events; similarly, watershed slope and aspect alone were not able to predict which watersheds would experience larger turbidity responses to precipitation events. Despite seeing significant differences from July to September, during runoff from May to June, there were no significant differences in turbidity between burned and unburned watersheds. These results indicate that drivers of sedimentation in these burned watersheds, for example erosive soils, were more susceptible to precipitation than snowmelt due to exposure to rain splash and the higher intensity precipitation associated with convective rainfall. We also note that if summers continue to extend in the western U.S., burned watersheds with steep slopes, poor vegetation recovery, and erosive soils may experience longer periods of increased sedimentation. Results from this work provide insight on characteristics that determine vulnerability to sedimentation after a wildfire and can help guide land managers in developing effective mitigation strategies.

TABLE OF CONTENTS

LIST OF FIGURES

LIST OF TABLES

ACKNOWLEDGMENTS

I would like to thank my family and friends for their support throughout this process, specifically my partner Mattie Hannigan, for her bottomless patience. I would like to thank my advisor, Dr. Kamini Singha, for sticking with me and mentoring me throughout graduate school, in addition to sharing her unwavering enthusiasm for all things hydrology. I would also like to thank my committee members, Dr. Terri Hogue and Dr. Brian Ebel, for providing data and sharing alternative perspectives, as well as Dr. Ashley Rust, for sharing data and her invaluable insight into the study area. I would like to recognize Steve Belz of Black Creek Hydrology and the Colorado Department of Water Resources for collecting and providing precipitation and discharge data following the West Fork Complex Fires. I would also like to acknowledge Abbye Neel, who provided Google Earth Engine code that greatly reduced the processing time associated with analyzing large EVI files.

CHAPTER 1
INTRODUCTION

In the western United States, wildfires are natural occurrences that are expected to increase in both frequency and severity in the coming decades (e.g., Westerling et al., 2006). Wildfires often decrease water quality in streams and rivers downstream of burned areas, which in turn affects downstream users, including wildlife and humans (e.g., Smith et al., 2011; Martin, 2016). Sediment loads are often elevated in streams located in recently burned areas (e.g., Neary et al., 1998; Ryan et al., 2011), which can have a detrimental effect on fish and other aquatic organisms (e.g., Rust et al., 2019) as well as downstream reservoirs and water management infrastructure (e.g., Fan et al., 1992). There are a number of factors that have been shown to influence the erodibility, and therefore sedimentation rates, in watersheds after wildfires (Moody et al., 2009). The quantity of sediment entering streams following wildfires is heavily influenced by the timing, duration, and intensity of precipitation events (e.g., Murphy et al., 2015), coupled with watershed slope, aspect, soil type, vegetation, ground cover, and burn severity. To explore the effects of these watershed characteristics on sedimentation post-fire, I analyzed sedimentation trends in seven watersheds, four burned and three unburned, in the Rio Grande headwaters following the 2013 West Fork Complex (WFC) fires (Figure 1.1).

Turbidity was previously collected in each of the seven watersheds from May-September of 2015 and 2016 (Rust et al., 2019). Using a variety of non-parametric statistical techniques, I analyzed watershed characteristics, including slope, aspect, soil type, burn severity, and vegetation recovery, which are commonly associated with post-wildfire erosion, in conjunction with turbidity to explore the connection between geological and ecological watershed characteristics and sedimentation. The goal of this work was to create a framework capable of assessing the vulnerability of watersheds to future problems associated with sedimentation, such as fish kill and damage to water management infrastructure, following wildfires based on watershed characteristics. While no single watershed characteristic studied was fully responsible for sedimentation trends, precipitation was shown to affect turbidity in watersheds differently based on

time of year, burn severity, and the erodibility of the soil. My work may assist watershed managers identify streams vulnerable to increases in turbidity and sedimentation following wildfires in areas with similar geological and ecological properties to the upper Rio Grande basin. For example, if a watershed experiences a low snowpack in the years following a wildfire, water managers can expect snow to have melted out of the watershed earlier in the season, leaving the burned watershed susceptible to precipitation-driven erosion for the duration of spring and summer. We could then expect higher turbidity, and therefore higher sediment concentrations, for a longer portion of the year, making streams in burned areas less habitable to fish and other aquatic organisms.

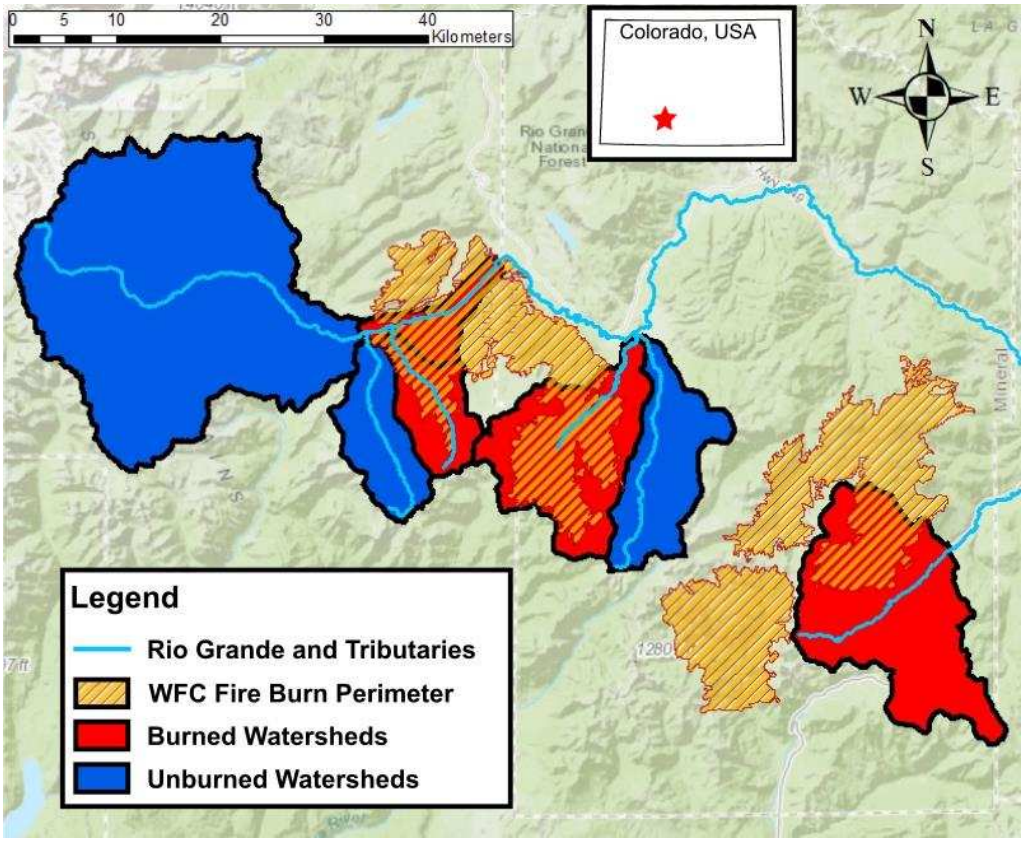

Figure 1.1: Study area in southwest Colorado near the West Fork Complex fires, which burned over 400 km^2 in 2013. The four watersheds selected for the study that were burned by the fires are denoted in blue. The three watersheds selected that were not burned by the fires are denoted in red.

CHAPTER 2

ANALYSIS OF WATERSHED PARAMETERS CONTROLLING TURBIDITY FOLLOWING THE WEST FORK COMPLEX FIRE

2.1 Abstract

In this work, we explore watershed characteristics associated with increased turbidity following wildfires, with the goal of developing relations between turbidity and slope aspect, soil type, slope, and vegetation health from the 2013 West Fork Complex Fire (WFC) in southwest Colorado, USA. Turbidity, precipitation, and stream discharge were measured from May to September in 2015 and 2016 in seven watersheds, four burned and three unburned. Slope, slope aspect, soil type, vegetation, precipitation, and burn severity were characterized for each of the seven watersheds, as well as inside the burned areas of the four burned watersheds. Turbidity was used in each watershed as the dependent variable.

Results indicate that from July to September of both 2015 and 2016, burned watersheds had larger spikes in turbidity following precipitation events than unburned watersheds. Higher burn severity and poor vegetation recovery were associated with the strongest positive correlations between total storm volume and turbidity responses. Enhanced Vegetation Index (EVI) was not consistently correlated with watersheds that experienced elevated turbidity following precipitation events. Watershed slope and aspect alone were not strong predictors of which watersheds would experience larger turbidity responses to precipitation events. During snowmelt driven runoff from May to June, no significant difference in turbidity between burned and unburned watersheds was found. These results indicate that drivers of turbidity in these burned watersheds, for example erosive soils, were more susceptible to precipitation than snowmelt due to exposure to rain splash and the higher intensity precipitation associated with convective rainfall. We also note that if summers continue to extend in the western U.S., burned watersheds with steep slopes and other relevant characteristics may experience longer periods of increased turbidity. Results from this work provide insight on characteristics that determine vulnerability to turbidity after a wildfire and can help watershed managers

predict future wildfire impacts on water quality, the health of aquatic organisms, and water treatment infrastructure.

2.2 Introduction

Wildfires are a natural occurrence in the western United States that can bring destructive changes to water quality in burned areas. Streams in burned areas often experience increased water temperature and decreased dissolved oxygen concentrations (e.g., Crouch et al., 2006) as well as increased levels of nutrients (Smith et al., 2011; Bladon et al., 2014; Hallema et al., 2018; Rust et al., 2018), all of which affect fish, wildlife, agriculture, and human consumption (e.g., Smith et al., 2011; Martin, 2016; Rust et al., 2019). Wildfires also increase the amount of sediment entering streams from burned watersheds (e.g., Moody et al., 2001; Ryan et al., 2011; Smith et al., 2011; Lucas-Borja et al., 2019), which can impact water quality and habitat for fish and other aquatic organisms (e.g., Lyon et al., 2008; Rust et al., 2019). Increased sediment loads can also cause operational problems for downstream reservoirs (e.g., Fan et al., 1992; Bladon et al., 2014). Predicting the impact of wildfires on sedimentation—and consequently water quality and the need for mitigation strategies to prevent issues like fish kill—remains difficult.

The erodibility of a watershed after wildfire depends on a number of factors, including ground cover, rainfall intensity, slope, native soil type, and burn severity (e.g., Debano, 2000; Miller et al., 2011; Moody et al., 2013; Sankey et al., 2017). The initial increase in sedimentation post fire is primarily caused by the change in vegetative cover and soil type following a burn (Pierce et al., 2004; Moody et al., 2013; Niu et al., 2014). After a forested area experiences a moderate- to high-severity burn, soil containing organic material often forms a layer of hydrophobic soil at or near the ground surface, accelerating erosion for a few years post-fire due to decreased soil infiltration and increased overland flow (e.g., Debano, 2000). On top of the hydrophobic layer of soil, burned organic litter and vegetation is left as a layer of ash, which is easily mobilized by precipitation due to the increased overland flow and can be a major source of sedimentation immediately following wildfires (e.g., Debano, 2000; Hassan et al., 2005). Burn-affected slopes above 15 percent are generally more susceptible to erosion, acting

as a “critical slope” for post-fire sedimentation (Pierson et al., 2007). Soil-water storage and slope failures following precipitation events have also been linked to slope aspect (Ebel et al., 2015; Perreault et al., 2017). Because southern aspects in the northern hemisphere often experience lesser snowpacks than northern aspects due to sun exposure and evaporation (e.g., Lopez-Moreno et al., 2014), snow often melts completely from southern aspects earlier in the year and produces less runoff than northern aspects. Vegetation cover type and density also strongly impact a hillslope’s susceptibility to erosion (Pierce et al., 2004; Ryan et al., 2011; Niu et al., 2014). Pre-burn vegetation can affect the size and severity of wildfires (e.g., Niu et al., 2014; Jones et al., 2017; Loomis et al., 2018), while post-burn vegetation recovery can reduce erosion and sedimentation (e.g., Lane et al., 2006; Kim et al., 2008). Slope and precipitation are also dominant controls on erosion toward streams; intense periods of precipitation following a wildfire are perhaps the largest catalysts for post-fire sedimentation (Lane et al., 2006; Ryan et al., 2011; Niu et al., 2014; Murphy et al., 2015), and effects are coupled with watershed slope, aspect, soil, and vegetation. Watershed sedimentation models, such as the Watershed Erosion Projection Project (WEPP), also rely on watershed characteristics such as climate, topography, and soil type to predict the amount of sediment from a given watershed into its surface waters (USDA-ARS National Soil Erosion Research Laboratory, 2017).

Due to land development, climate change, and historic wildfire suppression in forests, wildfires in the western U.S. are expected to continue to increase in both frequency and severity in coming decades (e.g., Neary et al., 1998; Westerling et al., 2006; Moritz et al., 2014; Sankey et al., 2017). Higher severity burns, along with droughts associated with climate change, are causing vegetation in burned areas to recover even more slowly after fire (Pierce et al., 2004), which will promote higher sediment yields during non-burned years (e.g., Ryan et al., 2011; Sankey et al., 2017). Pre-fire fuel treatment has shown to provide a worthwhile return on investment in terms of both fire suppression costs as well as damage to infrastructure downstream (Jones et al., 2017). However, the efficacy of fuels mitigation, given more frequent and severe wildfires and slower vegetative recovery in burned areas, is unknown (Pierce et al., 2004).

In the current study, we explore controls of sedimentation on seven distinct watersheds in the Rio Grande headwaters following the 2013 West Fork Complex (WFC) fires. Our work builds off prior studies, including Lane et al. (2005), in which sediment loads in two paired, burned, watersheds—one logged and one unharvested before the fire—were analyzed by correlating changing land cover, precipitation measurements, and soil properties to sediment loads before and after the fire. Others have similarly compared the effect of precipitation and streamflow on sedimentation between burned and unburned watersheds (e.g., Kunze et al., 2006; Silins et al., 2009; Wilson et al., 2018). Here, we expand beyond these papers analyzing sedimentation in watersheds at different times of the year, namely during peak snowmelt when turbidity is often elevated (e.g., Silins et al., 2009) and the summer convectional rainfall season after peak snowmelt. We also introduce slope, aspect, and size and severity of burn to expand on watershed characteristics associated with sedimentation and to identify watersheds vulnerable to increased sedimentation following wildfires We use non-parametric statistical tools to explore controls on turbidity —as a proxy for sedimentation—as the dependent variable. Turbidity, along with discharge and precipitation data, were collected in seven watersheds in and around the WFC fires in 2015 and 2016 (Rust et al., 2019). Spatial watershed characteristics thought to control sedimentation, such as burn severity, terrain, soil, and vegetation characteristics, were considered independent variables and characterized for each watershed using publicly available remotely sensed and ground-based data. Our goal was to explore geological and ecological watershed characteristics associated with post-fire sedimentation to determine whether a predictive index for future sedimentation problems in streams can be established and assist watershed managers in preparing for the impact of increased sedimentation on water quality, aquatic organisms, and water management infrastructure. The Colorado Water Conservation Board, which oversees funds allocated to watershed projects around the state, has allocated funds for wildfire recovery and risk mitigation in burned watersheds around Colorado; however, the most effective risk mitigation methods are still uncertain (Smith, 2021). This project looks to help quantify key watershed characteristics controlling increased sedimentation in Colorado watersheds.

2.3 Site Description

The data analyzed in this project comes from seven watersheds in the San Juan and Rio Grande National Forests in south-central Colorado (Figure 2.1). The Windy Pass, West Fork, and Papoose Fires, collectively known as the WFC fire, burned approximately 44,110 hectares of primarily National Forest-managed lands (Schroder, 2013), 63% of which was burned at a moderate to high severity. All fires were ignited by lightning strikes in early June, 2013 and burned into November of 2013 (Yochum et al., 2014). The WFC fire burned drainages of several tributaries to the Rio Grande River, as well as the main Rio Grande watershed itself (Yochum et al., 2014). Firefighting efforts managed to prevent the fire from spreading into several drainages, providing an opportunity to study the effects of the WFC fire by creating paired drainages of burned and unburned watersheds with similar geology and ecology.

The geology in the area is largely dominated by ash-flow deposits, with some alluvial deposits and igneous intrusions (Schroder, 2013). Soils are largely loamy with large rock fragments and covered by organic litter, which was removed by the WFC fire and increased the erodibility of the remaining soil in burned areas (Schroder, 2013). Vegetation in the WFC area consists primarily of spruces (*Picea*) and firs (*Abies*), many of which had already been killed by spruce beetles before the WFC fire (Schroder, 2013). At higher elevations near ridgelines, forbs, shrubs, and willows are present, while lower elevations near the Rio Grande floodplain are populated by stands of ponderosa pine (*Pinus ponderosa*) and Douglas-fir (*Pseudotsuga menziesii*) surrounded by riparian grasses, willows, and sedges (Schroder, 2013).

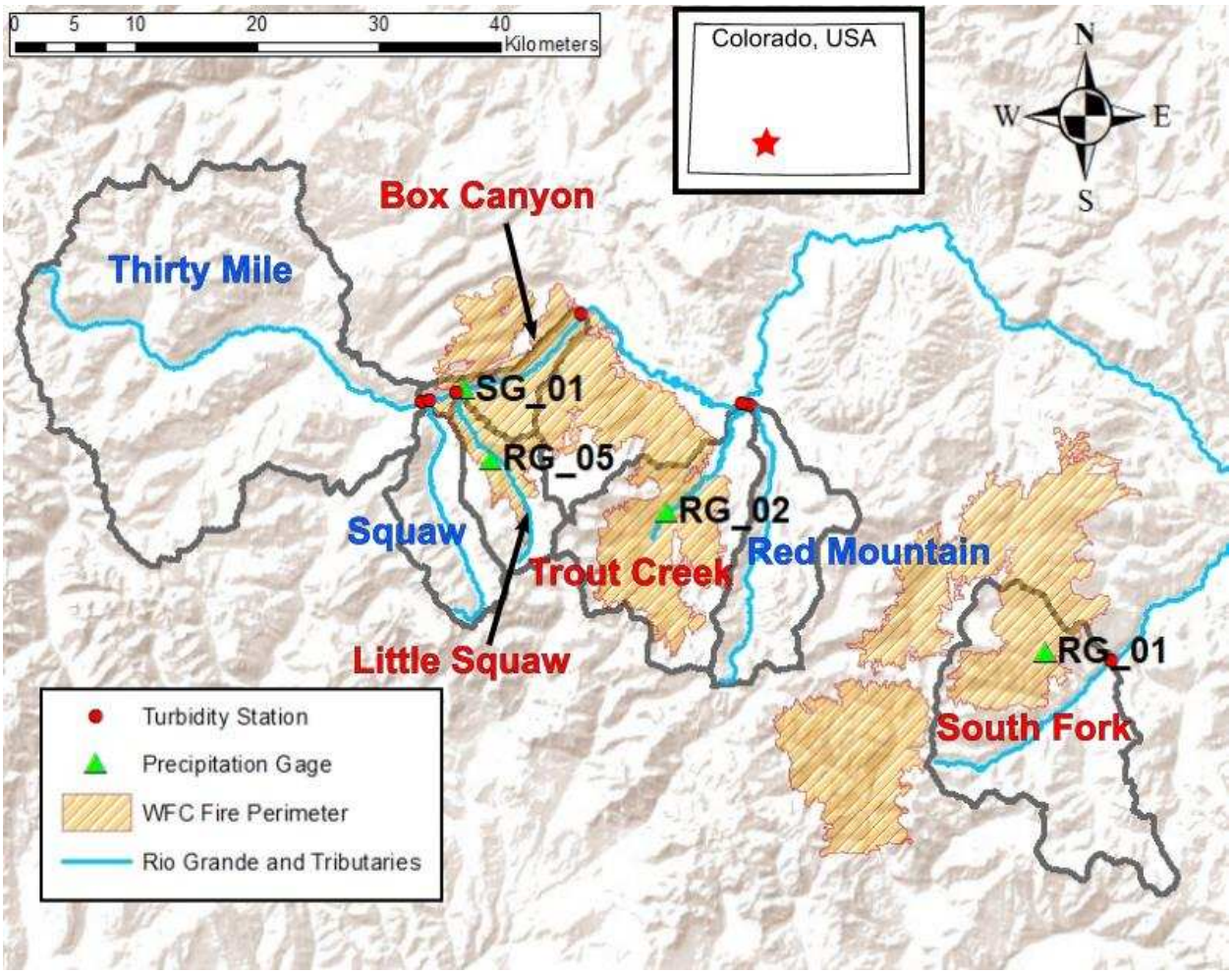

Figure 2.1: Study area including the seven selected watersheds near the West Fork Complex Fire. Four watersheds (Box Canyon, Little Squaw, Trout Creek, and South Fork) were burned, while three watersheds (Thirty Mile, Squaw, Red Mountain) were relatively unscathed. This creates three pairs of adjacent basins, one burned and one unburned, with Box Canyon/Thirty Mile, Squaw/Little Squaw, and Trout Creek/Red Mountain. Turbidity gauging stations are located at the outflow of each respective watershed. The South Fork of the Rio Grande watershed is located in the southeastern portion of the study area and is a different branch of the Rio Grande, isolated from the other watersheds in the study area. Burned watersheds are labeled in red, unburned watersheds are labeled in blue.

Rust et al. (2019) found that turbidity was higher in burned tributaries post wildfire, including Little Squaw, Trout Creek, and South Fork, when compared to measurements taken from the main stem of the Rio Grande, where flow is sourced from both burned and unburned watersheds. To mitigate the influence of water from

unburned watersheds diluting turbidity in burned areas located lower on the main stem of the Rio Grande, we selected seven watersheds for this study: Thirty Mile, Box Canyon, Squaw, Little Squaw, Trout Creek, Red Mountain, and South Fork (Figure 2.1). Of the seven watersheds, four were burned by the WFC fires—Box Canyon, Little Squaw Creek, Trout Creek, and South Fork of the Rio Grande watersheds—and three—Thirty Mile on the Rio Grande, Squaw Creek, and Red Mountain Creek—were not. Squaw and Little Squaw watersheds as well as Red Mountain and Trout Creek watersheds are tributaries to the Rio Grande adjacent to one another, providing two pairs of otherwise similar burned and unburned watersheds. Thirty Mile and Box Canyon are also paired basins, although turbidity in both watersheds was measured in the main stem of the Rio Grande, which means turbidity measured at the Box Canyon station cannot be entirely isolated from turbidity originating from the Thirty Mile basin above. The Thirty Mile gauge was also located less than a mile downstream of the Rio Grande Reservoir, which may have impacted turbidity measurements at that site.

2.4 Watershed Data and Analyses

To evaluate the impact of watershed characteristics on post-fire sedimentation and the effectiveness of their use as sedimentation predictors, characteristics commonly associated with sedimentation were selected based on previous research (Table 2.1; e.g., Miller et al., 2011; Chin et al., 2016; Sankey et al., 2017; Hallema et al., 2018; Lucas-Borja et al., 2019). Variables that were spatially and temporally variant throughout the study area and study period, from May through September of 2015 and 2016, include precipitation, stream flow, vegetation, and the dependent variable, turbidity. Independent variables for each watershed that were spatially variant but temporally static over the study period include watershed slope and aspect, soil type, and burn severity (Table 2.1).

Kruskal-Wallis tests, one-way non-parametric ANOVAs on rank, were used to verify whether watersheds were statistically different from than one another based on a variety of data, including slope, burn severity, and vegetation cover. If the Kruskal-Wallis test results suggested that there were watersheds statistically different from the rest, a Dunn's non-parametric multiple comparison test (Dunn, 1964) was conducted to identify

which watershed(s) were significantly different from the others. Because of the large sample size provided by the 10m DEM pixel-based analysis (n > 100,000), Cohen's d was used to calculate the effect size in the terrain datasets (Hollander et al., 1973).

In the seven selected watersheds, turbidity was measured from May through September in both 2015 and 2016 by Rust et al. (2019). Discharge was measured continuously throughout the study period at three of the seven watersheds—Thirty Mile, Box Canyon, and South Fork—by the Colorado Division of Water Resources. Four precipitation gages, placed by Black Creek Hydrology and the Colorado Division of Water Resources, were chosen to represent paired watersheds based on their geographic proximity (Figure 2.1). We characterized land cover using NASA's MODerate Resolution Imaging Spectroradiometer (MODIS) 8-day average Enhanced Vegetation Index (EVI). The time-invariant variables, which include terrain characteristics, soil properties, and burn severity distribution from the WFC fire, were calculated at the smallest sub-watershed resolution possible (details in Table 2.1) based on available data and summarized by using average and maximum values for both the entire watershed and the areas inside the burned perimeter using ArcGIS. To separate how turbidity responded to snowmelt versus precipitation, turbidity in each watershed was analyzed in conjunction with other watershed characteristics over three distinct periods of time: during snowmelt (May-June), post-snowmelt (July-September), and over the entire summer (May-September) in both 2015 and 2016.

Table 2.1: Data used for the statistical tests, including dependent and independent variables, the data format and source, a description of those data, and their spatial/temporal scale. Turbidity, precipitation, and discharge were collected from May-September of 2015 and 2016. Watershed abbreviations: BC – Box Canyon, TM – Thirty Mile, SQ – Squaw, LS – Little Squaw, TC – Trout Creek, RM – Red Mountain, SF – South Fork.

Parameter/ Data Type	**Data Source**	**Information Provided**	**Spatial/Temporal Scales**
Turbidity (NTU—dependent variable)	Rust et al., 2019	Proxy for sedimentation	7 stations, 15-minute intervals at TM, BC, SF; 3-hr intervals at SQ, LS, TC, RM
Fire Severity	Monitoring Trends in Burn Severity (MTBS)	Impact of wildfire severity on sedimentation	30-m resolution, time invariant
Terrain (Digital Elevation Model)	USGS 3D Elevation Program (3DEP)	Slope and other terrain features as a predictive index for sedimentation with and without fire	10-m resolution, time invariant
Soil (Hydrologic Soil Grouping)	Gridded Soil Survey Geographic Database (gSSURGO)	Soil erodibility as a predictive index for sedimentation with and without fire	10-m resolution, time invariant
Land Cover (Enhanced Vegetation Index)	MODerate Resolution Imaging Spectroradiometer (MODIS)	Existing vegetation as a predictive index for sedimentation with and without fire	250-m resolution, 8-day intervals
Precipitation (Volume and Storms)	Rust et al., 2019; Black Creek Hydrology	Annual precipitation and precipitation intensity as a predictive index for sedimentation with and without fire	4 stations, 10-minute intervals
Discharge	Rust et al., 2019; Colorado Division of Water Resources	Sediment volume calculations; Discharge as a predictive index for sedimentation with and without fire	3 stations, 15-minute intervals at TM, BC, SF

2.4.1 Burn Severity

To quantify the effect of a fire on vegetation, the change or delta in normalized burn ratio (dNBR) is calculated by subtracting the post-fire NBR value from the pre-fire NBR value for each pixel, which gives an index for fire severity and vegetation response for a given wildfire at a 30-m pixel scale (MTBS, 2020). The Monitoring Trends in Burn Severity (MTBS) program—an interagency program supported by the U.S. Geological Survey Center for Earth Resources Observation and Science and the USDA Forest Service Geospatial Technology and Applications Center—has compiled GeoTIFF raster layers for a pre-fire image, post-fire image, NBR, dNBR, and Thematic Burn Severity for almost every wildfire in the U.S. since 1984, all of which are freely available to the public. Using the dNBR values calculated, the MTBS produces a Thematic Burn Severity raster layer that quantifies burn severity as high, moderate, low, and unburned for each pixel based on historically calibrated dNBR values and interagency generated post-fire Burned Area Emergency Response reports (Miller et al., 2015; Tran et al., 2018). Burn severity is defined as the organic matter consumption from fire above and below ground (Keeley, 2009). On the ground, burned areas that experience a loss of surface litter but maintain a healthy soil organic layer and living trees are considered to have been burned at a low severity, while areas burned at a moderate- to high-severity experience canopy cover loss, extensive damage to the soil organic layer, and in some cases complete loss of vegetative cover (Keeley, 2009). Because the dNBR values have shown to accurately distinguish fire severity classes (e.g., Tran et al., 2018), the Thematic Burn Severity GeoTIFF layer calculated using the dNBR was used here to classify burn severity for numerical analysis of the burned watersheds. The percent areas burned at high, moderate, low, and unburned severities were calculated for each watershed individually by counting the pixels from the Thematic Burn Severity layer at each severity level in the watershed compared to the total number of pixels in the watershed.

2.4.2 Terrain

We calculated the distribution of four terrain characteristics using built-in ArcGIS spatial analyst tools: 1) average slope, 2) percent of watershed that was south facing (as a measure of aspect), 3) percent of watershed above 15% critical slope (e.g.,

Pierson et al., 2015) and 4) percent of watershed above 33-degree critical slope (DiBiase et al., 2020). These four terrain characteristics were also calculated for the portion of the watershed inside the burn perimeter in each of the four burned watersheds to isolate the effect of terrain characteristics on burned areas.

To verify differences in slope and aspect between watersheds or burned portions of watersheds, Kruskal-Wallis tests were run using the DEM 10-m pixels as samples for each watershed using a = 0.05 as the significance level; tests returning a p-value less than 0.05 allow us to reject the null hypothesis of equality. Watersheds with a calculated Cohen's d/effect size of less than 0.2 were considered invariant, regardless of the significance of difference calculated by the Kruskal-Wallis tests.

2.4.3 Soil Type

Soil runoff potential was determined by the gSSURGO Hydrologic Soil Group classification system, which rates soil on a scale from A to D, where soils with a high infiltration rate and therefore a lower runoff potential are classified as A and soils with a slower infiltration rate and therefore a higher runoff potential are classified as D. Soils with lower infiltration rates (e.g. type C and D) are commonly associated with increased erosion and therefore sedimentation (de Dios Benavides-Solorio, 2003; Pierson et al., 2007; Hallema et al., 2017).

The area of each soil type was summed in each watershed to calculate the distribution of soil types. Areas with unknown or undefined soil type ratings encompassed less than 3% of the total area in each of the seven watersheds, and therefore were ignored. Dual-classified soils, for example A/D, describe soils in an area for drained and undrained scenarios. These soils were classified according to their undrained rating in all of the seven watersheds due to the typical conditions found in the WFC study area (Yochum et al., 2014).

2.4.4 Vegetative Cover

NASA's MODIS provided 8-day composite Enhanced Vegetation Index (EVI) was used to analyze the WFC study-area watersheds due to its sensitivity to densely vegetated areas and varying canopy structures (MODIS, 2020). Possible EVI values

range from -2,000 to 10,000, and provide information on Leaf Area Index and chlorophyll production, which are associated with vegetation health (MODIS, 2020). While higher EVI values are associated with more dense, green vegetation, thresholds for what is considered healthy is dependent on vegetation type and climate (e.g., Jarchow et al., 2018).

The seasonal average EVI, maximum EVI, and recovery of EVI were calculated in each watershed as well as inside the fire perimeter of burned watersheds using data from May-September 2015 and 2016. Average EVI was calculated using the mean of all EVI values measured during these times and over these areas of interest. The maximum EVI values were based on the average of maximum pixel values in each watershed over every 8-day sweep. This seasonally averaged maximum EVI value allowed us to compare values measured post-fire in 2015 and 2016 to pre-fire values. Pre-fire average and maximum EVI values were calculated using data from May-September over a five-year period from 2008-2012 to account for natural variability. EVI recovery was calculated using both average EVI and maximum EVI by taking the difference in post-burn average and maximum EVI and the pre-burn values. Recovery was calculated relative to each area's pre-fire EVI averages regardless of vegetation type or density compared to other watersheds to identify trends in vegetation health. Burned areas with seasonal average and maximum EVI values near or higher than pre-burn conditions were considered recovered. EVI "recovery" was also calculated for unburned areas and compared to the burned areas' recovery to verify the change in burned areas was due to vegetation recovery and not seasonal variation from more favorable growing conditions. Kruskal-Wallis tests were used to confirm significant differences between EVI in each watershed.

2.4.5 Precipitation

Precipitation was measured using temporary un-heated tipping bucket rain gages installed in the field by the Colorado Division of Water Resources (CDWR) and Black Creek Hydrology Consultants after the WFC fires. These temporary stations were placed near the turbidity sensors (Figure 2.1) and recorded incremental precipitation every 10 minutes from May to October of both 2015 and 2016 (Rust et al., 2019). RG01

was chosen to represent the South Fork watershed due to its location in the center of the watershed. RG02 was chosen to represent both the Trout Creek and Red Mountain watersheds, RG05 was chosen to represent the Squaw and Little Squaw watersheds, and SG01 was chosen to represent the Thirty Mile and Box Canyon watersheds based on proximity. To maintain consistency between measurements at different sites, nearby permanent Snow Telemetry (SNOTEL) sites were ignored; only the temporary precipitation gauges installed by the CDWR and Black Creek Hydrology consultants were used.

Storms were analyzed along with local turbidity measurements to determine how responsive turbidity was in each of the watersheds. Storms were identified using the inter-event time definition method available in the IETD package in R. To do so, the program sums continuous precipitation data over time, marks the start of a rain event as the first non-zero precipitation measurement following a previous storm, and marks the end of the rain event by the final precipitation measurement before a dry-gap, or zero-precipitation measurement window. Rain events that meet a user-defined total volume, maximum intensity, and dry-gap (i.e., no precipitation measured) minimum threshold are classified as a storm. Moody and Martin (2001) identified a precipitation threshold of 5 mm/hr for sediment production in a burned watershed on the Front Range of Colorado, and classified precipitation falling harder than 10 mm/hr for 30 minutes as a high-intensity event. Consequently, precipitation events that measured at least 5 mm of rain and were separated from other precipitation events by at least 10 “dry” hours were categorized as storms for each of the four precipitation gauges throughout the study period. The total precipitation volume; total duration; average precipitation intensity; and I-10 peak precipitation intensity, defined by the largest single 10-minute precipitation measurement recorded during a storm, were calculated for each storm for each precipitation gage individually.

2.4.6 Turbidity

Turbidity was used as a proxy for sedimentation. While relations between total suspended solids (TSS) concentrations and Nephelometric Turbidity Units (NTUs) vary based on particle size, shape, and source, as well as dissolved organic carbon and

other properties affected by the geology of the contributing watershed (e.g., Downing, 2006), TSS concentrations and turbidity in NTUs are linearly correlated up to 2000 NTUs in both natural and engineered water systems (Lane et al., 2006; Al-Yaseri et al., 2013; Rügner et al., 2014). Turbidity data were collected for all seven watersheds from May to October of 2015 and 2016 using 3000-NTU maximum detection-limit turbidity sensors on Hydrolab MS5 multiparameter water quality sondes (Rust et al., 2019). Turbidity was measured instantaneously at 15-minute intervals in the South Fork, Box Canyon, and Thirty Mile and at 3-hour intervals in the Red Mountain, Trout Creek, Squaw, and Little Squaw watersheds, and were calibrated every two weeks (Rust et al., 2019).

Mean and median turbidity measurements were calculated in each watershed for the entire season. Turbidity responses following storms in each watershed were calculated using the difference between the highest turbidity measured during or immediately after a storm and the median turbidity measurement observed from 3 days before the start of the storm through the three days following the end of the storm. Due to variation in storm length, these observation periods were not identical in length, but were used to encapsulate three full diurnal cycles before and after the storm. To separate turbidity spikes caused by storms from baseline turbidity fluctuations, turbidity responses that were less than 33% of the weekly median turbidity measurement were not considered responses, based on variability noted above, and recorded as a response of 0 NTUs. Later in the summer, when smaller diurnal turbidity fluctuations occasionally exceeded 33% of the weekly median due to decreased weekly median turbidity values, turbidity responses to storms were easier to identify due to the lower baseline turbidity and were verified manually to exceed the diurnal turbidity fluctuations.

Statistical tests were used to explore differences in turbidity over the system, and how turbidity was related to storms. Kruskal-Wallis tests were conducted on turbidity responses calculated in each watershed in 1) 2015 and 2016, to compare how the turbidity response to precipitation in watersheds changed over time; as well as 2) between burned and unburned watersheds and 3) between watersheds inside the burned and unburned groups respectively, to explore whether there were significant

differences between systems due to natural variability versus the impacts of fire. Dunn's tests were used on datasets that were identified as statistically different by the Kruskal-Wallis tests to identify the individual watersheds with a statistically different turbidity response to storms. A Pearson's correlation coefficient and p-value were also calculated for each watershed between turbidity response and total storm volume, storm length, average intensity, and peak I-10 intensity individually. Correlation coefficients were calculated both pre- (May-June) and post-snowmelt (July-September) in both 2015 and 2016. In addition to the individual watersheds, correlations were also calculated between groups of burned and unburned watersheds. For groups of burned and unburned watersheds, Pearson's correlation was also calculated between turbidity response to storms and maximum EVI recovery, mean EVI recovery, percent of the watershed above 33-degrees, average slope, percent of the watershed burned at a moderate-high severity, percent of the watershed with soil type A, and percent of the watershed with north-facing slopes in addition to the storm characteristics tested in individual watersheds. For burned watersheds, the terrain and vegetation characteristics were calculated using the area inside the burned perimeter, while terrain and vegetation characteristics in the unburned watersheds were calculated over the entire watershed. Correlations with a p-value greater than 0.05 were considered statistically insignificant.

2.5 Results

2.5.1 Burn Severity

The percent of each watershed burned by the WFC fire was calculated using the MTBS burn severity layer (Figure A.2). The WFC fire was found to have burned less than a half of a percent of the area of the three unburned watersheds: Thirty Mile, Squaw, and Red Mountain. Of the four burned watersheds, Box Canyon was found to have burned over the largest percentage of its total watershed area, with moderate to high severity burning over more than half of the watershed (Figure 2.2A). Looking inside the burned perimeters of the four burned watersheds (Figure 2.2B), ~75% of the South Fork burned area was burned at a high and moderate-to-high severity, more than the other watersheds; Box Canyon and Trout Creek experienced ~60% moderate-to-high severity burn inside their burned areas, ~20% of which was high severity, while Little

Squaw's burn was the least intense, with only 50% at a moderate-to-high severity (Figure 2.2B).

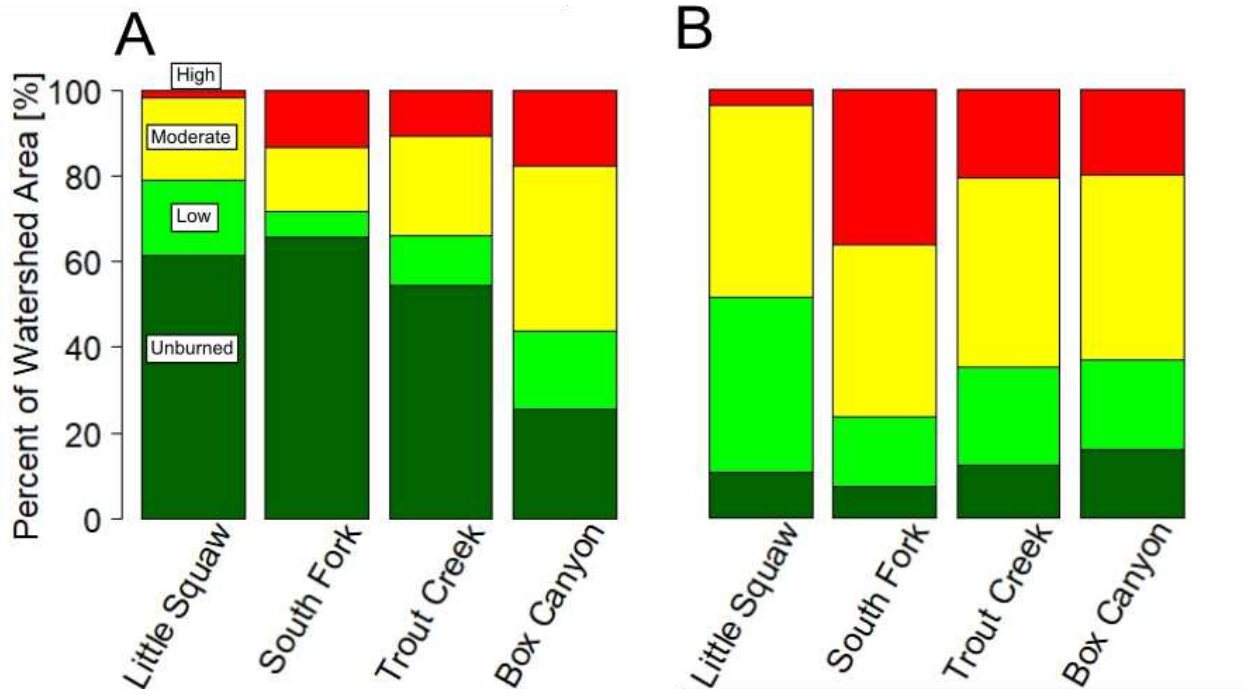

Figure 2.2: Percent of (A) watershed and (B) the area inside the fire perimeter in burned watersheds that are considered unburned (dark green), burned at low (light green), moderate (yellow), and high (red) severity according to the MTBS burn severity map, ordered from lowest percent of watershed area burned at a moderate to high severity to highest. Overall, Little Squaw experienced the smallest percentage of watershed area burned at a moderate to high severity, while Box Canyon experienced the largest. Inside the burned perimeter, Little Squaw experienced the smallest percentage of area burned at a moderate to high severity, while South Fork experienced the largest.

2.5.2 Terrain

Despite statistically significant differences found between overall slope distributions measured in the seven watersheds (p-value < 2.2e-16; machine precision), there was little variation in average slope or percent of watershed above critical slopes. Only the watershed with the lowest average slope, Little Squaw, showed non-negligible effect sizes ($d > 0.2$) when compared to the two watersheds with the highest average slope, Squaw ($d = 0.26$) and Red Mountain ($d = 0.22$), suggesting that differences in slope between the watersheds at this scale are minimal. Box Canyon had the lowest percent area with a southern aspect (~35%; Kruskal-Wallis, p-value < 2.2e-16; $d = 0.5$)

of all seven watersheds; the Thirty Mile and South Fork basins had the highest percent area with a southern aspect, both near 50% (Figure 2.3A; Kruskal-Wallis, p-value < 2.2e-16; d = 0.2).

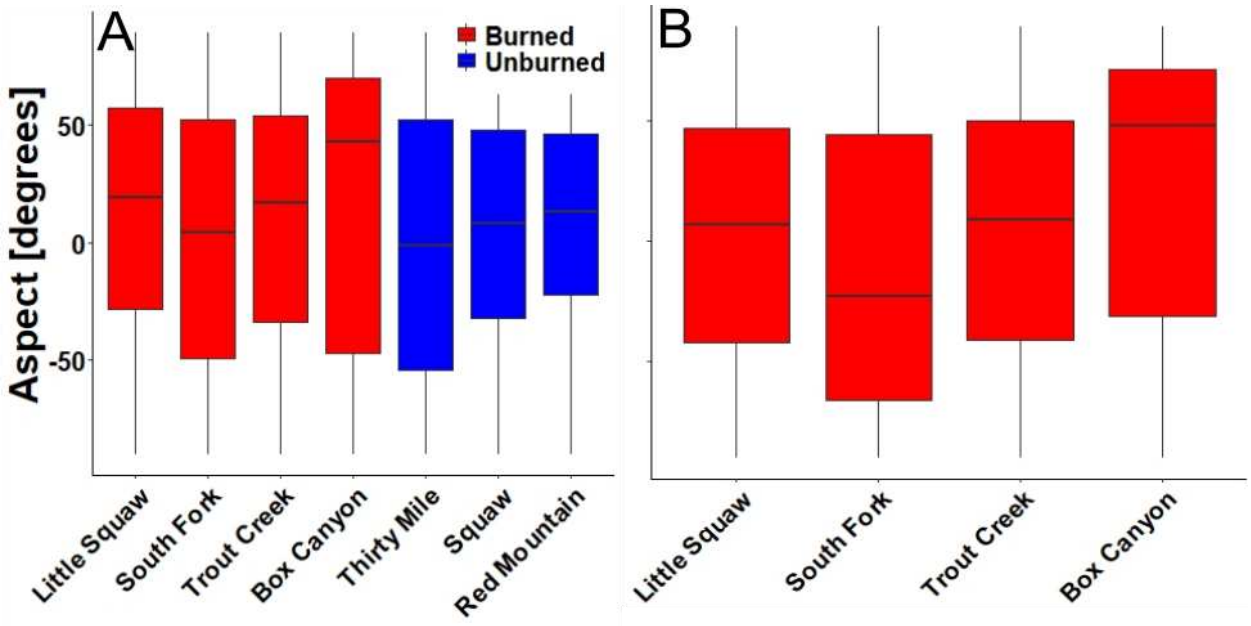

Figure 2.3: Distributions of aspect measured at a 10m resolution over (A) the entire watershed and (B) the area inside the burned perimeter of the burned watersheds. Aspect here is depicted as degrees from east or west, with 90 being due north and -90 being due south. All watersheds contained more north-facing slopes than south-facing (A). Inside the burned perimeters, south Fork was the only watershed with more area south-facing (~58%) than north-facing. The burned area inside Box Canyon was had the most area north-facing (~70%) (B). Red fill denotes burned watersheds, blue fill denotes unburned watersheds.

Terrain characteristics were also calculated for the area inside the burn perimeters for each burned watershed (Figure 2.3B). Inside the burned areas, South Fork had the largest percentage of its area south-facing (~58%; Kruskal Wallis, p-value < 2.2e-16; d = 0.4), while Box Canyon had the smallest percentage of its area south-facing (~30%; Kruskal-Wallis, p-value < 2.2e-16; d = 0.4). Distributions of slope measured in each of the four burned areas were considered to be statistically different from one another (Kruskal-Wallis, p-value < 2.2e-16); however, small effect sizes (d < 0.2) suggest that the statistical significance found using the Kruskal-Wallis tests were

influenced by a large sample size and little variation in watershed slope exists between the burned areas of the burned watersheds.

2.5.3 Soil Type

Among all seven watersheds, Thirty Mile had the largest percentage of its area dominated by type D soils, which are the most prone to erosion (Figure 2.4A). Trout Creek and Box Canyon, both burned watersheds, contained the highest percentage of type A soils, which allow more infiltration and therefore are less prone to erosion (Figure 2.4A). In addition to classifying soil types in the seven watersheds as a whole, soil types were classified inside the fire perimeter of the four burned watersheds (Figure 2.4B). Trout Creek's burned area contained almost 80% type A soil, the highest percentage of all burned watersheds, while South Fork and Little Squaw's burned areas contained around 40% soil type A. The burned areas inside all four burned watersheds contained less than 5% type D soil, while all but Box Canyon contained ~10% type D soil throughout their entire watershed.

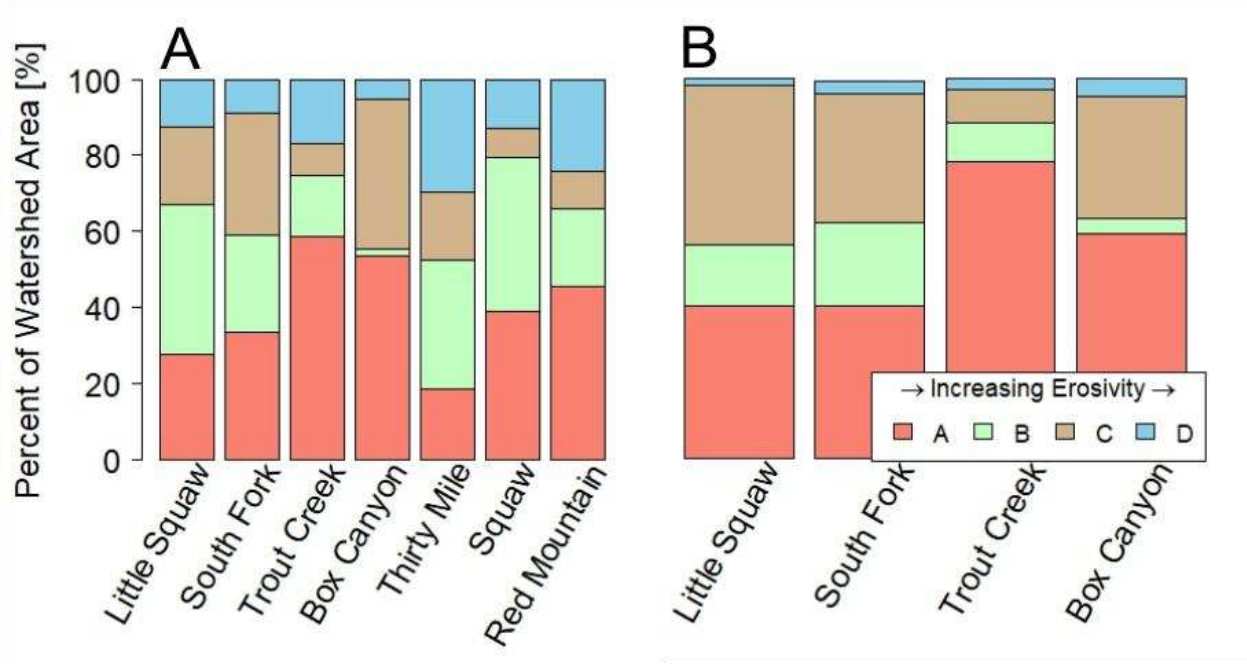

Figure 2.4: Percentages of soil types classified by SSURGO soil surveys inside (A) each of the seven watersheds and (B) the area inside the fire perimeter in burned watersheds. Soil identified as type A allow the most infiltration and therefore less erosion, whereas type D soils are associated with less infiltration and therefore more erosion.

2.5.4 Vegetative Cover

We compared seasonal average EVI and maximum EVI for all seven watersheds in 2015 and 2016 to earlier, pre-fire conditions from 2008-2012. All watersheds except Red Mountain (unburned) and Box Canyon (burned) had lower seasonal mean EVI in 2015 when compared to pre-fire conditions (Figure 2.5A). In 2016, all watersheds had a higher seasonal mean EVI than in 2015, although Thirty Mile (unburned) and Trout Creek (burned) both experienced lower seasonal mean EVI than pre-fire conditions (Figure 2.5A). All watersheds had a higher maximum EVI in 2015 than pre-fire (Figure 2.5B).

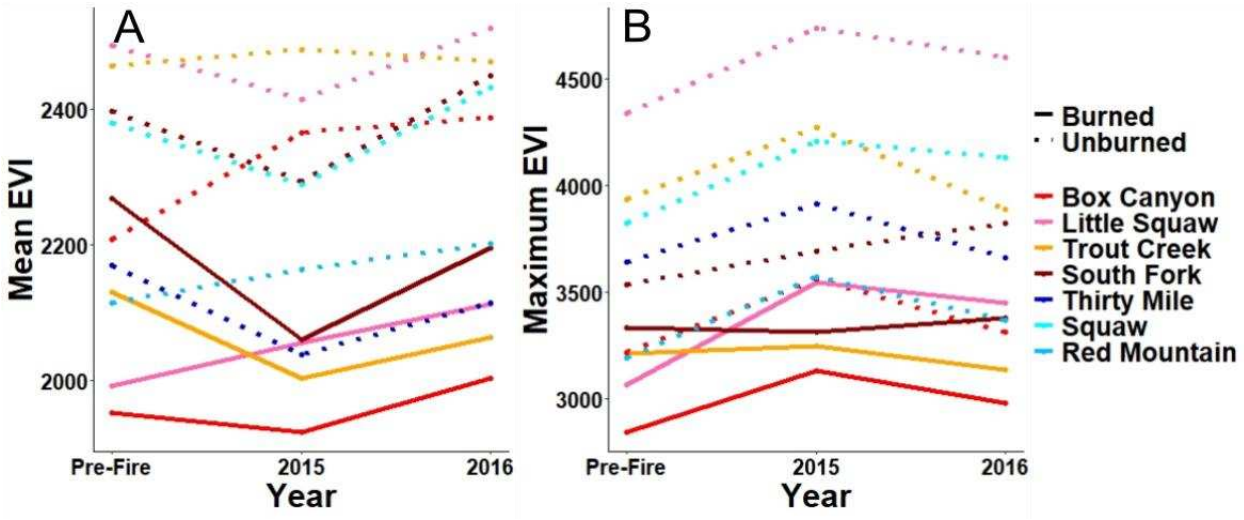

Figure 2.5: (A) Mean EVI and (B) maximum EVI measured in all seven watersheds inside the burned perimeter (solid line) and outside the burned perimeter (dashed line). Pre-fire values were calculated using an average of mean and maximum values measured from May-September of 2008-2012 for both the burned and unburned portions of the watersheds. Burned watersheds are in warm colors, unburned in cool colors.

Results for the pre- and post-burn seasonal average and maximum EVI within the burned perimeters in each of the four burned watersheds show the recovery of the burned areas specifically (Figure 2.5). Of the four burned watersheds, the only watershed that experienced recovery to pre-fire average EVI values in 2015 was Little Squaw. All four burned watersheds' seasonal average EVI increased in 2016 from 2015; Box Canyon also recovered to pre-burn conditions in 2016, but Trout Creek and

South Fork did not. In 2015, the maximum EVI inside the burned areas were higher than pre-fire conditions in three of the four burned watersheds, excluding the South Fork basin. In 2016, the maximum EVI in the burned area of the South Fork basin increased to be higher than pre-fire conditions (Figure 2.5B).

2.5.5 Precipitation

We compared total precipitation (Table A.1) and average storm volume (Figure 2.6; Table A.1) between watersheds from May-September of 2015 and 2016. Trout Creek/Red Mountain received more total precipitation from May-September in 2015 than Box Canyon/Thirty Mile (Dunn's test, p-value = 4.1e-13) and South Fork (Dunn's test, p-value = 6.5e-21). Squaw/Little Squaw also received more total precipitation in 2016 than Box Canyon/Thirty Mile (Dunn's test, p-value = 6.8e-10) and South Fork (Dunn's test, p-value = 1.2e-16) but was not significantly different from Trout Creek/Red Mountain (Dunn's test, p-value = 0.27). There was no significant difference in median storm volume between watersheds in 2016 (Figure 2.6B; Kruskal-Wallis, p-value = 0.55).

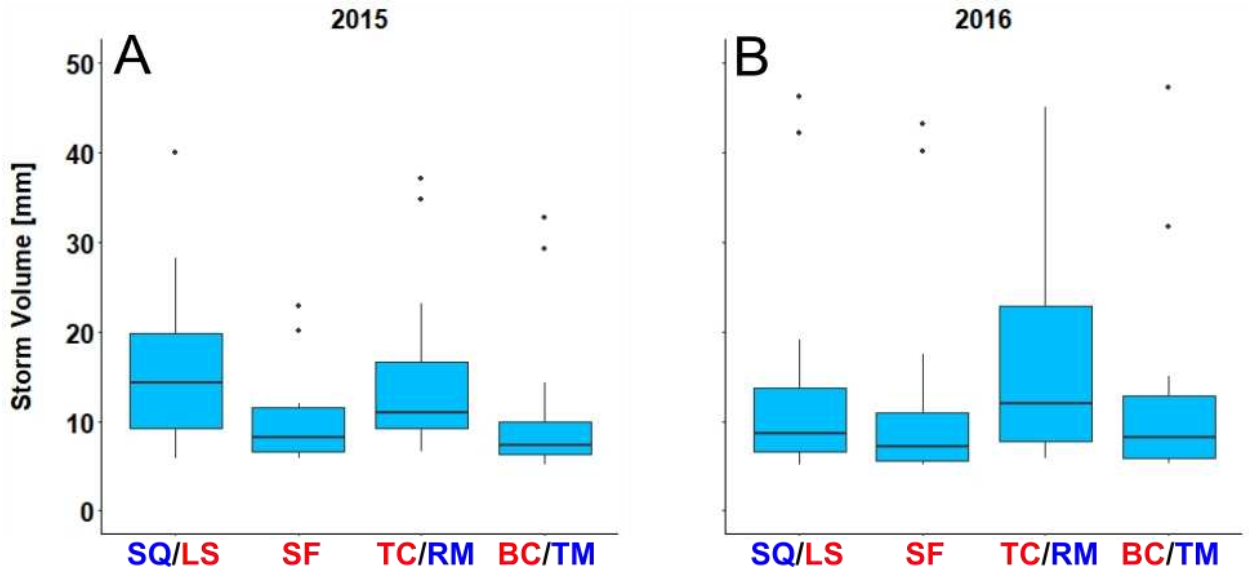

Figure 2.6: Total precipitation fallen during storms identified from May-September of (A) 2015 and (B) 2016 for Squaw/Little Squaw (SQ/LS), South Fork (SF), Trout Creek/Red Mountain (TC/RM), and Box Canyon/Thirty Mile (BC/TM). A single rain gauge was used to characterize precipitation in paired basins. Burned watersheds are labeled in red, unburned watersheds are labeled in blue.

2.5.6 Turbidity

2.5.6.1 Diurnal Fluctuations in Turbidity

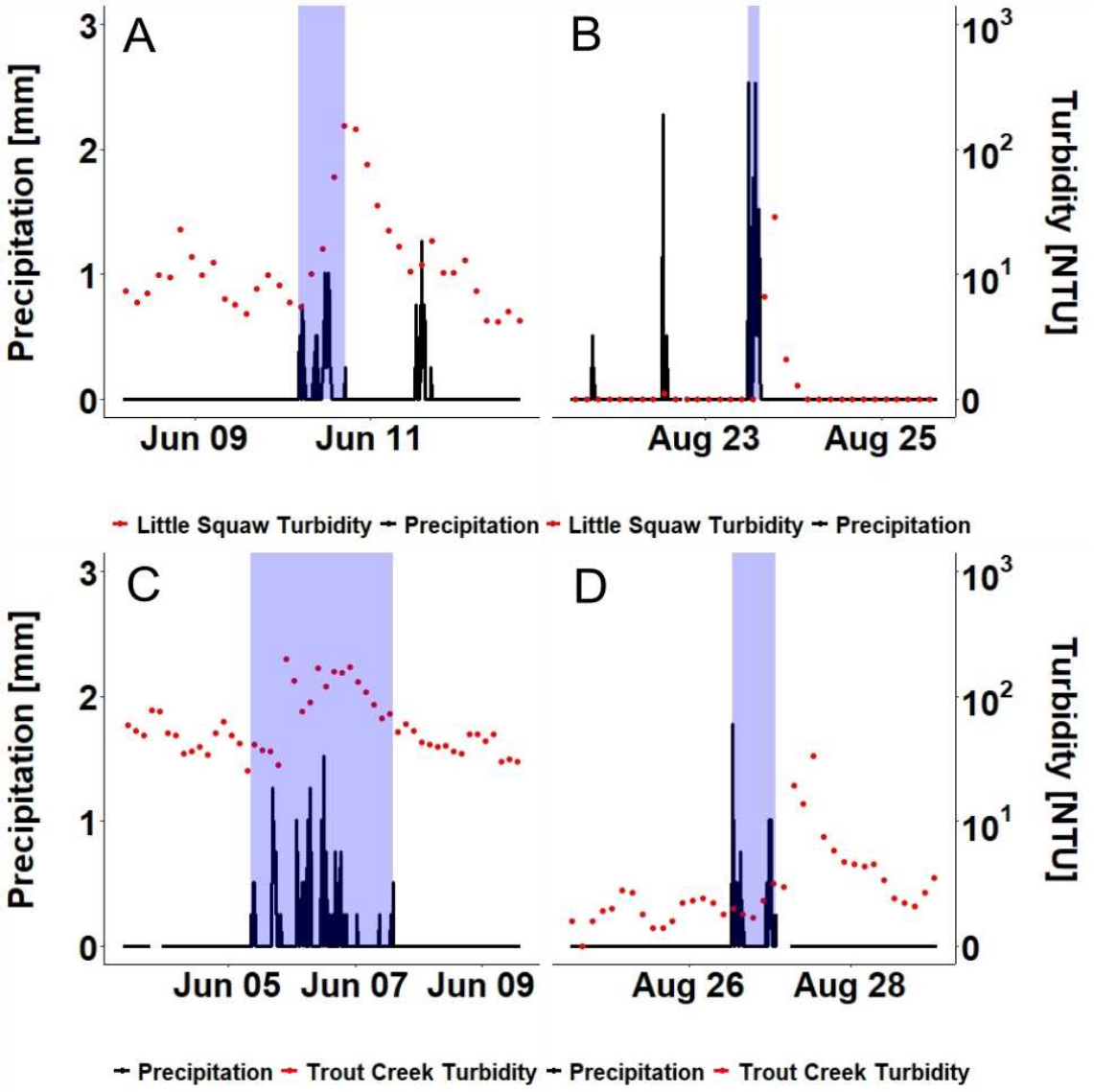

Figure 2.7: Diurnal fluctuation and storm response of turbidity in 2015 during snowmelt for fire-impacted sites (A) Little Squaw and (C) Trout Creek, as well as later in the summer after snowmelt had subsided for (B) Little Squaw and (D) Trout Creek. The duration of each storm is shaded in blue. Baseline turbidity is high in both watersheds during snowmelt (A and C) compared to the later part of the summer (B and D). During snowmelt, the turbidity response to precipitation was generally more apparent in (A) Little Squaw than in (C) Trout Creek, despite experiencing less total precipitation.

Turbidity in the WFC study area fluctuated on a diurnal cycle throughout the year, but particularly during the spring snowmelt, with turbidity ranging as much as 600 NTUs between the middle of the night and mid-afternoon when snowmelt is highest (Figure 2.7A). When turbidity and flows were highest, from late May to early July, most watersheds saw a daily fluctuation in turbidity of +/- 33% from the daily mean turbidity during periods of low or no precipitation (Figure 2.7A and Figure 2.7B). Later in the summer, most watersheds experienced smaller diurnal turbidity fluctuations, of less than 10 NTUs, between mid-night to mid-afternoon (Figure 2.7C and Figure 2.7D).

2.5.6.2 Baseline/Average Turbidity

When comparing average turbidity between paired basins during snowmelt (May-June) of 2015, two of the three paired basins (Thirty Mile/Box Canyon and Squaw/Little Squaw) saw higher average turbidity and standard deviation in turbidity in the unburned watershed than the paired burned watershed (Figure 2.8A; Table A.3). Post-snowmelt (July-September) of 2015, however, all three burned watersheds had higher average turbidity and standard deviation in turbidity than their unburned paired watershed (Figure 2.8B; Table A.3). During snowmelt in 2016, the only paired watersheds where the unburned watershed experienced higher turbidity than the burned watershed was Squaw/Little Squaw (Figure 2.8C; Table A.3). Transitioning to post-snowmelt in 2016, a similar trend to what was observed in 2015 occurred; burned watersheds experienced higher average turbidity and standard deviation in turbidity than they had experienced during snowmelt, with the exception of South Fork (Figure 2.8D; Table A.3).

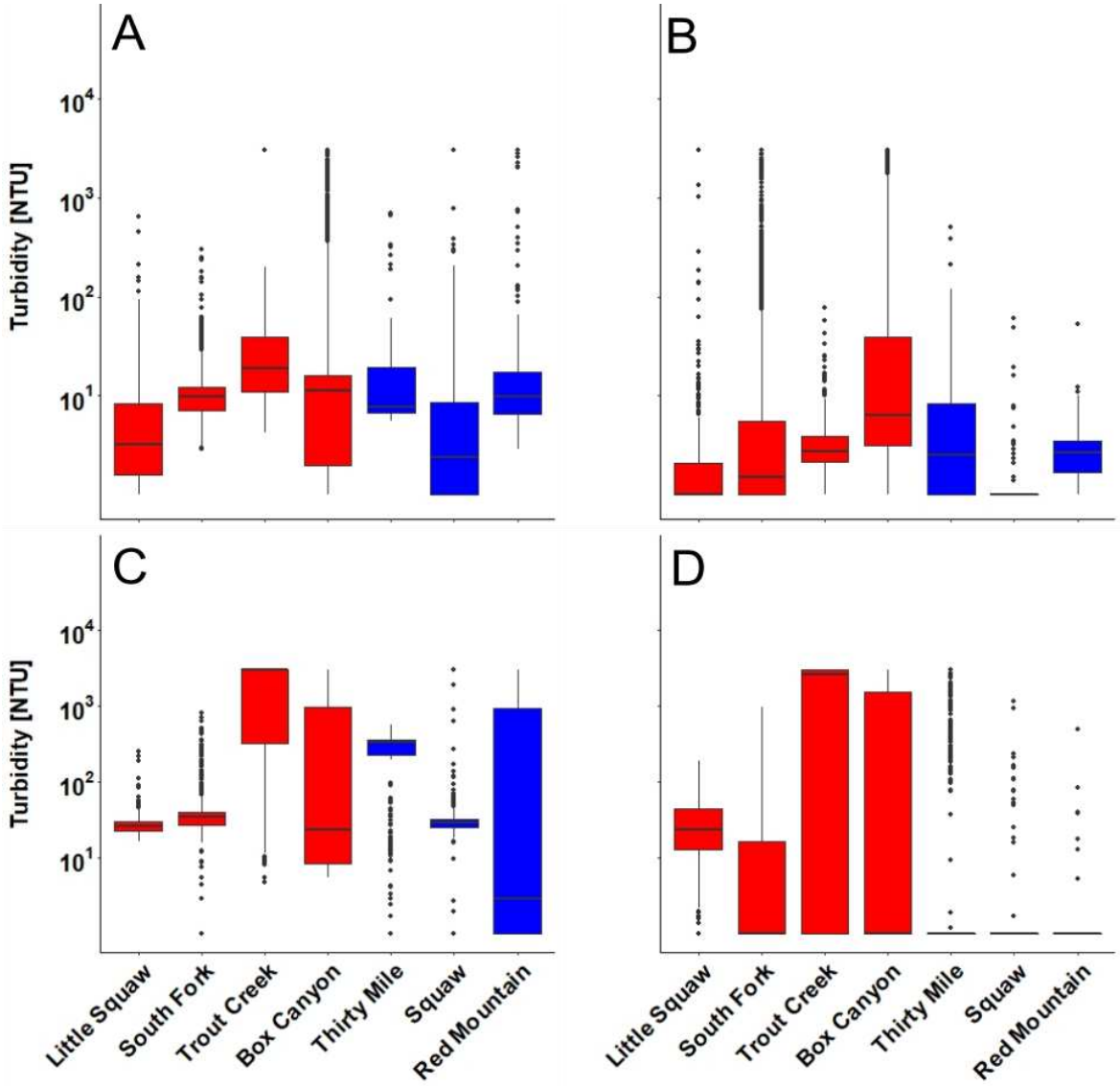

Figure 2.8: Turbidity measurements during (A) snowmelt (May – June) of 2015, (B) post-snowmelt (July – September) of 2015, (C) snowmelt of 2016, and (D) post-snowmelt of 2016. Turbidity was higher in 2016 than 2015 for most watersheds. Burned watersheds are colored red, while unburned watersheds are colored blue. Burned watersheds often experienced higher median turbidity measurements post-snowmelt, while turbidity in unburned watersheds decreased from snowmelt to post-snowmelt. *Turbidity data in South Fork was only collected through August in 2015.

To explore how streamflow and turbidity varied in relation to each other, log10 turbidity was plotted against log10 stream discharge in the three watersheds where discharge was measured: Thirty Mile (unburned), Box Canyon (burned), and South Fork (burned; Figure 2.9). A regression slope near zero would indicate that turbidity remains

constant as discharge varies, as has been explored in concentration-discharge relations of solutes (e.g., Godsey et al., 2009; Hunsaker et al., 2017). Negative slopes are caused by increasing discharge coinciding with decreasing turbidity, and would indicate that increased flows are diluting the sediment concentrations. Positive slopes suggest that turbidity increases more quickly than discharge. In 2015, both South Fork (slope = 0.94 ± 0.01, r^2 = 0.51) and Thirty Mile (slope = 0.85 ± 0.01, r^2 = 0.40) showed positive regression slopes. In 2016, all three watersheds with discharge data showed positive regression slopes (South Fork slope = 0.90 ± 0.01, r^2 = 0.37; Thirty Mile slope = 1.68 ± 0.02, r^2 = 0.27; Box Canyon slope = 0.90 ± 0.03, r^2 = 0.06). This result indicates that in each of these three watersheds, two of which were burned and one of which was unburned, increases in stream discharge were always associated with increases in turbidity. All regression slopes were found to be significantly different from zero (p-value < 2.2e-16; machine precision; Table A.4).

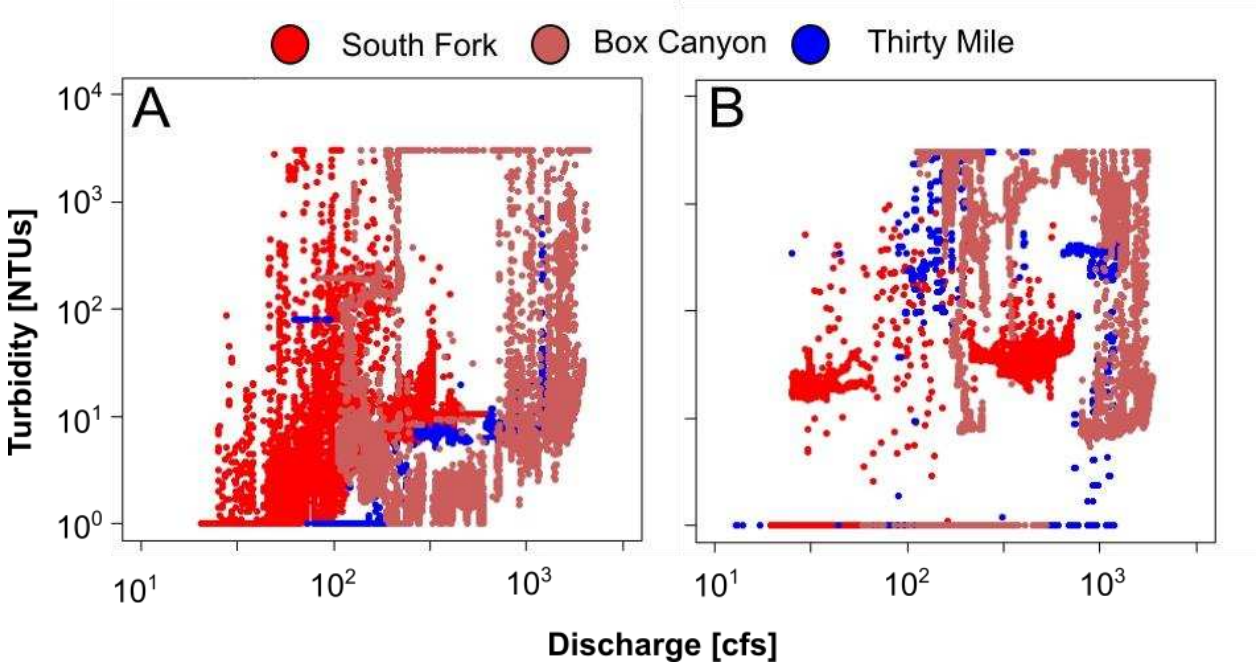

Figure 2.9: Log10-turbidity – log10-discharge plots from the South Fork, Box Canyon, and Thirty Mile watersheds from May-September of (A) 2015 and (B) 2016. South Fork and Box Canyon, shown in two shades of red, were burned watersheds, while Thirty Mile, shown in blue, was unburned.

2.5.6.3 Turbidity Response to Storms

From May through September of 2015, 82% of storms triggered a turbidity response in all watersheds, while only 35% of storms triggered a turbidity response from May through September of 2016 (Table A.2). In 2015, storms triggered a turbidity response 91% of the time in burned watersheds compared to 70% of the time in unburned watersheds. In 2016, only 43% of storms triggered a response in burned watersheds and only 23% of the time in unburned watersheds. In 2015, turbidity responses in burned watersheds were higher than responses in unburned watersheds (Kruskal Wallis p-value = 0.004), especially in the South Fork basin (Figure 2.10A). In 2016, however, unburned watersheds experienced larger turbidity responses to storms than burned watersheds (Kruskal-Wallis, p-value 0.02), driven by the Thirty Mile and Squaw watersheds (Figure 2.10B).

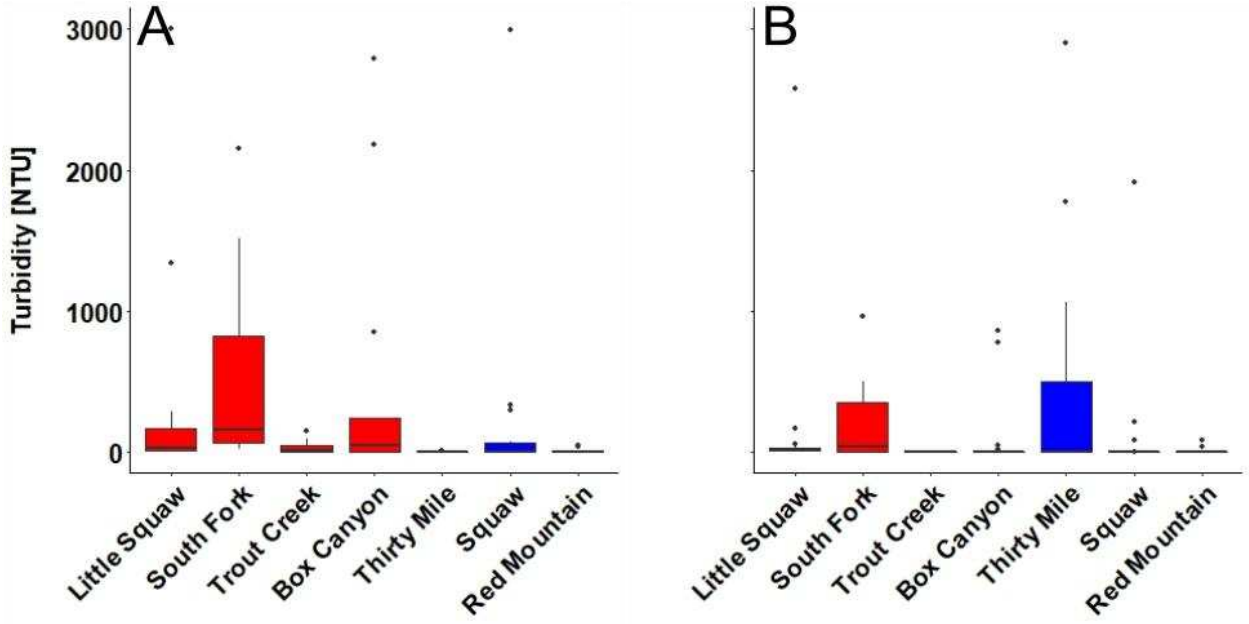

Figure 2.10: Distributions of turbidity responses to storms for all watersheds in (A) 2015 and (B) 2016 (B). Red box plots denote burned watersheds, blue denotes unburned watersheds. The four burned watersheds are listed in order of lowest percentage of watershed burned by the WFC fires (Little Squaw) to highest percentage (Box Canyon). In 2015, burned watersheds experienced larger turbidity responses to storms, while in 2016, unburned watersheds did.

There was no significant difference in the magnitude of turbidity responses to storms between burned and unburned watersheds from May-June of 2015 (Figure 2.11A; Kruskal-Wallis, p-value = 0.84) or 2016 (Figure 2.11C; Kruskal-Wallis, p-value = 0.13). Post-snowmelt (July-September) in 2015, burned watersheds experienced significantly higher turbidity responses to storms than unburned watersheds (Figure 2.11B; Kruskal-Wallis, p-value = 0.001). However, from July-September of 2016, large responses measured at the Thirty Mile gage drove unburned watersheds to have a higher turbidity response on average than burned watersheds (Figure 2.11D). Excluding results from Thirty Mile, burned watersheds experienced larger responses post-snowmelt in 2016 than unburned watersheds (Figure 2.11D; Kruskal-Wallis, p-value = 0.04).

Turbidity responses from July-September in 2015 (Figure 2.11B) were significantly higher in South Fork (median = 155 NTUs) than Box Canyon (median = 13 NTUs; Dunn's test, p-value = 0.02) and Trout Creek (median = 10 NTUs, Dunn's test, p value = 0.003), but not Little Squaw (median = 26.75 NTUs; Dunn's test, p-value = 0.09). From July-September of 2016, turbidity responses in Little Squaw (median = 12 NTUs) were significantly higher than Box Canyon (median = 0 NTUs; Dunn's test, p-value = 0.04), but not South Fork (Figure 2.11D; median = 0 NTUs; Dunn's test, p-value = 0.30). Trout Creek had no measurable turbidity responses in 2016. During the post-snowmelt portion of 2015, moderate to strong correlations were found between turbidity response and storm volume in two burned watersheds: Trout Creek (Pearson's R = 0.69, p-value = 0.01) and South Fork (Pearson's R = 0.89, p-value = 0.003), but not Box Canyon (Pearson's R = -0.16, p-value = 0.65) or Little Squaw (Pearson's R = 0.61, p-value = 0.06). Only one of those watersheds, South Fork (Pearson's R = 0.84, p-value = 0.001), maintained a strong correlation between turbidity response and total storm volume post-snowmelt in 2016.

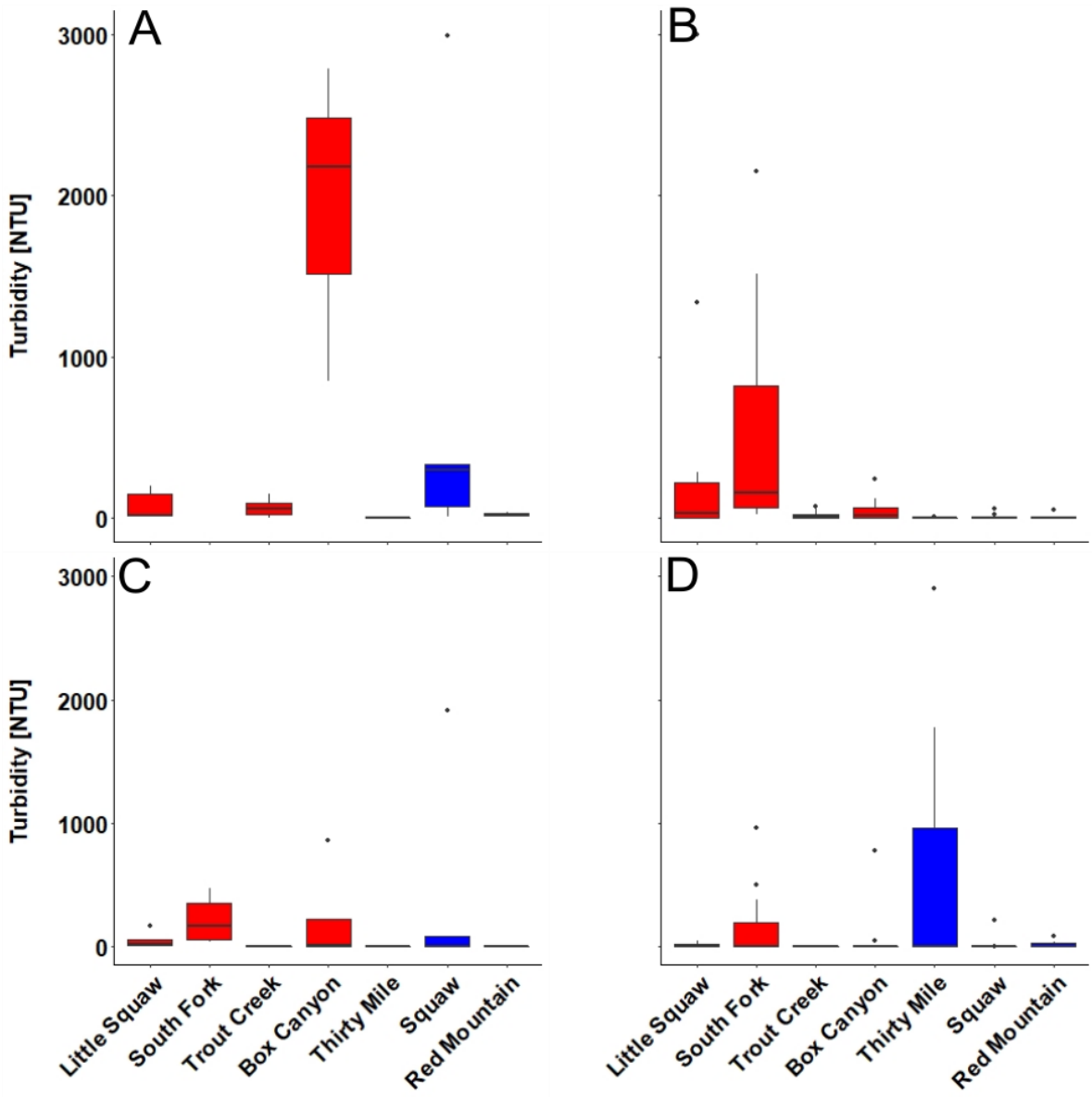

Figure 2.11: Rises in turbidity following storms in each watershed during (A) snowmelt (May-June) of 2015, (B) post-snowmelt (July - September) of 2015, (C) snowmelt of 2016, and (D) post-snowmelt of 2016. Red plots denote burned watersheds, blue plots denote unburned watersheds. The four burned watersheds are listed in order of lowest percentage of watershed burned by the WFC fires (Little Squaw) to highest percentage (Box Canyon).

2.5.6.4 Turbidity and Watershed Characteristic Correlations

In the four burned watersheds, few consistent and relevant correlations were found between watershed characteristics and turbidity (Figure 2.12). The turbidity

response to storms in all burned watersheds was found to be positively correlated to total storm volume (Pearson's R = 0.44, p-value = 0.02) and peak storm I-10 intensity (Pearson's R = 0.52, p-value = 0.004) during the post-snowmelt portion (July-September) of 2015, but not during any other time period (Figure 2.12). During the same time, the turbidity response to storms was also negatively correlated to the percentage of the burned area with soil type A, which is the soil type with the greatest infiltration capacity, during the post-snowmelt portion of 2015 (Pearson's R = -0.36, p-value = 0.04), meaning watersheds with less erosive soils experienced smaller spikes in turbidity following storms. The percentage of the area inside the fire perimeter burned at a moderate to high severity was also positively correlated to the turbidity response to storms in the burned watersheds during snowmelt (Pearson's R = 0.27, p-value = 0.02) and post-snowmelt (Pearson's R = 0.28, p-value = 0.04) of 2016, but not 2015.

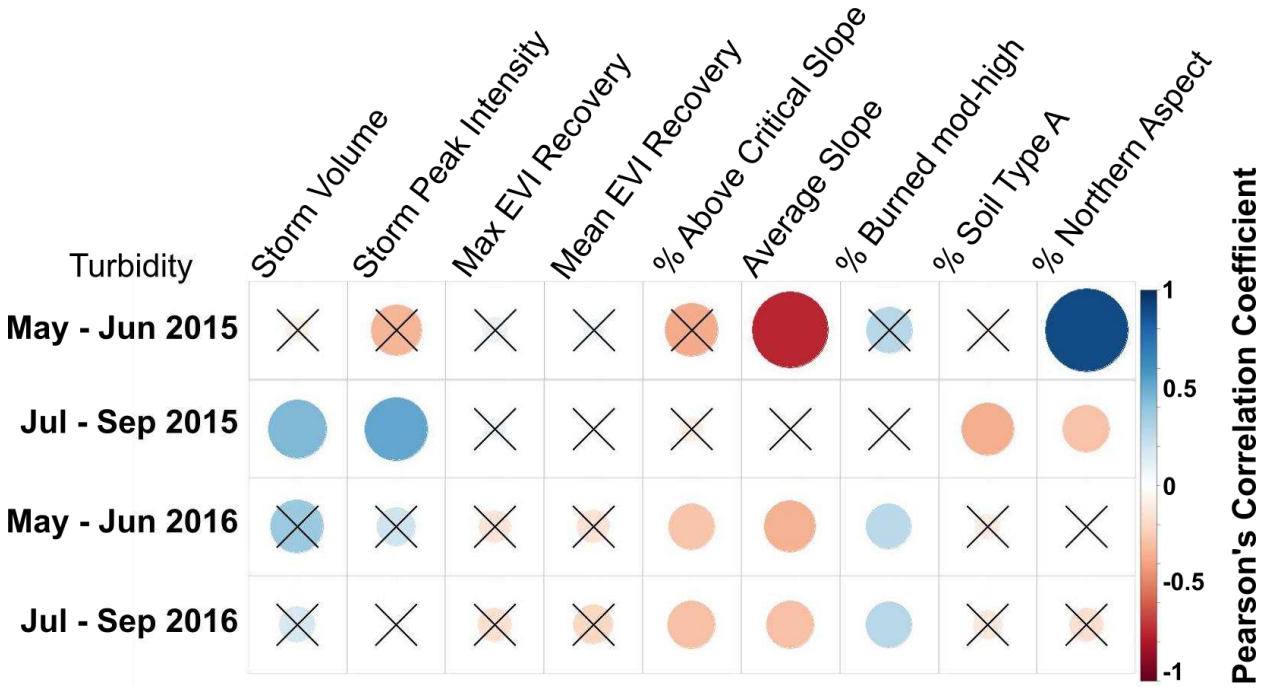

Figure 2.12: Pearson's correlations in the four burned watersheds between the turbidity response to storms and independent variables, including storm volume, storm peak intensity, maximum EVI recovery inside the burned perimeter, mean EVI recovery inside the burned perimeter, percent of the burned perimeter above the critical slope (33-degrees), average slope, percent of the burned area burned at a moderate to high intensity, percent of the burned area with soil type A, and percent of the burned area with a northern aspect. Blue indicates a positive correlation, red indicates a negative

correlation. The area of the circle is proportional to the correlation coefficient. X denotes the correlation was not statistically significant (p-value > 0.05).

In the three unburned watersheds, few significant correlations were found between any watershed characteristic and turbidity until the post-snowmelt portion of 2016 (Figure 2.13). (Figure 2.13). Unexpectedly, negative correlations were observed during the post-snowmelt (July-September) portion of 2016 between the turbidity response to storms and maximum EVI recovery (Pearson's R = -0.43, p-value = 0.003), mean EVI recovery (Pearson's R = -0.45, p-value = 0.0007), percent of the watershed above 33-degrees (Pearson's R = -0.38, p-value = 0.007) and average slope (Pearson's R = -0.44, p-value = 0.003). Negative correlations were also found between the turbidity response to storms and the percent of the watershed with a northern aspect (Pearson's R = -0.39, p-value = 0.001) and the percent of the watershed with soil type A (Pearson's R = -0.45, p-value = 6.0 e-5), which was consistent with results from the burned watersheds (Figure 2.12).

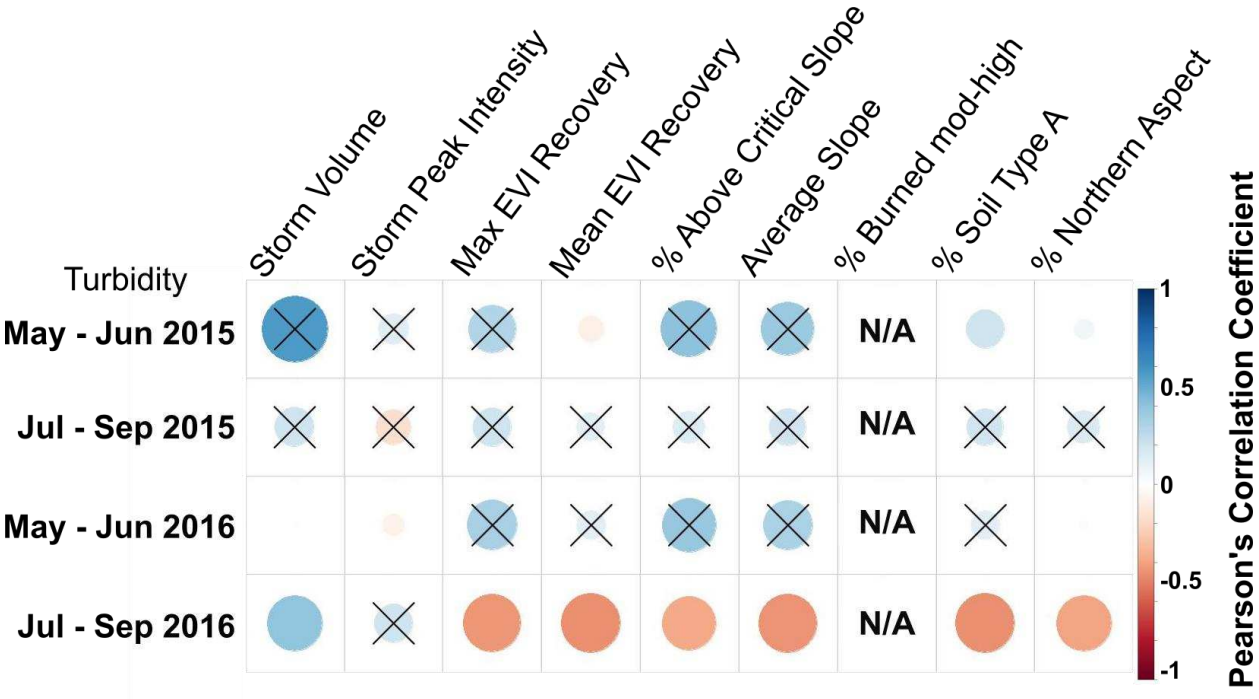

Figure 2.13: Pearson's correlations in the three unburned watersheds between the turbidity response to storms and independent variables, including storm volume, storm

peak intensity, maximum EVI recovery in the watershed, mean EVI recovery in the watershed, percent of the watershed above the critical slope (33-degrees), average slope of the watershed, percent of the watershed with soil type A, and percent of the watershed with a northern aspect. Blue indicates a positive correlation, red indicates a negative correlation. X denotes the correlation was not statistically significant (p-value > 0.05).

2.6 Discussion

Turbidity was higher in burned watersheds than unburned watersheds following the WFC fires (Figure 2.8, Figure 2.9, Table A.3), which is consistent with observations in other post-fire turbidity and sedimentation studies (e.g., Lane et al., 2006; Hohner et al., 2016; Rust, 2019). During snowmelt (May-June), turbidity in burned and unburned watersheds were similar or unburned watersheds experienced higher turbidity than their burned counterpart (Table A.3, Figure 2.8). Post snowmelt (July-September) in 2015, however, three of the four burned watersheds—Box Canyon, Little Squaw, and South Fork—experienced higher mean turbidity and standard deviation in turbidity than they did during snowmelt (May-June), while all unburned watersheds experienced lower turbidity and standard deviation in turbidity post-snowmelt (Figure 2.8). This result suggests that during the snowmelt-driven runoff, burned watersheds may not experience any more erosion than unburned watersheds. The difference in turbidity measured between burned and unburned watersheds was more apparent after the spring snowmelt had subsided (Figure 2.8). This result conflicts with results from previous studies, which found that post-wildfire sediment production primarily occurred during snowmelt (e.g., Silins et al., 2009; Wall et al., 2020). Others have found that increased snowmelt-driven erosion and sedimentation occurs during the first year after a burn event, but increased sedimentation is more noticeable following precipitation events later in the summer in subsequent years (Ryan et al., 2011; Murphy et al., 2015; Hallema et al., 2017). Turbidity and precipitation data were not collected in the WFC study area in 2014, the year following the WFC fire, so we cannot determine whether turbidity was elevated in the burned watersheds during the spring snowmelt in 2014, the first year following the fire; however, because storms triggered fewer turbidity responses in burned watersheds in 2016 than 2015 and turbidity in burned watersheds was lower

in 2016 than 2015, turbidity in our burned watersheds appears to be following similar downward trends to those identified by Ryan et al. (2011) and Hallema et al. (2017). This result suggests that the wildfire's impact on sedimentation diminishes with time.

We tested a variety of watershed characteristics, including burn severity, vegetative cover, slope, aspect, soil erosivity, and precipitation, to explore their relation to turbidity. Our original goal was to use multivariate regression as a tool to identify which watershed characteristics were associated with higher rates of sedimentation following the WFC fires, as has been done similarly following the Bobcat fire in Colorado (de Dios Benavides-Solorio, 2003; Kunze et al., 2006). The de Dios Benavides-Solario (2003) and Kunze et al. (2006) studies following the Bobcat fire in Colorado used small $1m^2$ plots on burned slopes to measure sedimentation following artificially simulated precipitation events, which provided 26 sediment collection points sourced from plots with unique watershed characteristics available for regression analysis. In our study, only four turbidity sensors were located at the base of burned watersheds, and each watershed encompassed a vast area including widely varying terrain, vegetation cover, burn severity, and soil types summarized across the entire watershed. Because of the limited number of turbidity monitoring sites available, we were unable to find statistically significant regression fits between any combination of watershed characteristics and turbidity. Consequently, we pull apart our relations individually below, as has been done in Australia (Lane et al., 2006) and Canada (e.g., Silins et al., 2009), both of which involved a small number of watersheds in the studies.

It is possible that the burned watersheds appeared more reactive to rain events later in the summer because their highly erosive soil is more exposed. In 2014, snow in the Rio Grande basin was observed to begin melting in early May, leaving little snow in all watersheds by the end of June (T. Hogue, observation, 2014). This reduction in snow cover coincides with the time of year we observe an increase in average turbidity (Figure 2.8B and Figure 2.8D) and turbidity responses to storms (Figure 2.11B and Figure 2.11D) in burned watersheds. During the post-snowmelt (July-September) portion of 2015, the strongest correlations between the size of the turbidity response and total storm volume were identified in all four burned watersheds (Figure 2.12).

During that same period of time, the turbidity response to storms in the burned watersheds also showed negative correlations to the percentage of the watershed with soil type A (Figure 2.12), suggesting that having more erosive soils (type B-D) exposed to precipitation from July-September in 2015 promoted higher rates of erosion and therefore sedimentation. The two burned watersheds that experienced the highest turbidity responses from July-September in 2015, South Fork and Little Squaw (Figure 2.11B), contained only ~40% Type A soil and generally more of the erosive Type B-D soil inside their burn perimeters than the other burned watersheds (Figure 2.10B). Similar results have been seen in other systems; once the ground is no longer covered by a protective layer of snow, watersheds can become more susceptible to raindrop splash-driven erosion, therefore increasing the role of vegetative cover and soil type in sedimentation following storms (Debano, 2000; Moody et al., 2013; Lucas-Borja et al., 2019). If reducing snowpack, earlier spring snowmelt, and delayed winters associated with climate change continue to elongate summers in the western U.S. (e.g., Bladon et al., 2014; Valentin, 2017), watersheds impacted by wildfire may experience unprotected soils for a longer portion of each year, resulting in more sedimentation for years following fire.

EVI recovery may not be a primary factor in determining which watersheds would experience higher rates of sedimentation in these systems, which conflicts with results from previous studies (Lane et al., 2006; Kim et al., 2008). The change in average and maximum EVI was largely not correlated to the magnitude of turbidity responses in 2015 or 2016 in burned or unburned watersheds (Figure 2.12 and Figure 2.13), suggesting that EVI recovery at this spatial or temporal scale does not accurately predict sedimentation rates in these watersheds post-fire alone. Little Squaw showed the highest mean and maximum EVI recovery inside the burn perimeter from pre-fire conditions of the burned watersheds in 2015, while South Fork showed the lowest in 2015 (Figure 2.5), despite South Fork experiencing larger turbidity responses to storms than all other watersheds except Little Squaw (Figure 2.11A). Both Little Squaw and South Fork experienced higher average EVI inside their burned perimeters in 2016 than 2015, indicating positive vegetation recovery (Figure 2.5A), which coincides with a decrease in average turbidity response in both watersheds post-snowmelt (July-

September) from 2015 to 2016 (Figure 2.11B and Figure 2.11D). This result suggests that positive EVI recovery is associated with a decrease in turbidity response to storms, which contradicts our previous results from 2015. It is possible that vegetation characteristics not captured well by EVI, such as vegetation type, which was used in the qualitative approach taken by Kim et al. (2008) to analyze the effect of vegetation recovery on soil conservation post-fire, may be better at predicting the effect of vegetation recovery on sedimentation post-wildfire. For example, the burned area in Little Squaw had a larger population of aspen trees (*Populus tremuloides*) than the other burned watersheds (Rust et al., 2019), which may provide higher EVI values earlier in the post-fire recovery process than other vegetation types, which could be interpreted as a relatively quick recovery from fire. This result would indicate that vegetation types that regrow quickly after wildfire and therefore provide some canopy cover from precipitation, such as aspens (*Populus tremuloides*), may provide a false sense of recovery when measured with EVI in terms of the ability to reduce sedimentation.

The severity of burn between watersheds did not appear to have a large direct effect on turbidity but did determine how quickly vegetation was able to recover. Only 49% of the area burned in Little Squaw was burned at a moderate to high severity, the lowest of the burned watersheds, while 76% of the area burned in South Fork was burned at a moderate to high severity, the highest of the burned watersheds. The large percentage of the burned area in the South Fork basin burned at a moderate to high severity may have played a role in the larger turbidity responses to storms in the South Fork basin (Figure 2.11), which had slow vegetation recovery. The relatively small percentage of the burned area in the Little Squaw basin burned at a moderate to high severity may have allowed vegetation to recover more quickly, resulting in smaller albeit consistent turbidity responses to storms in 2016 (Figure 2.11B). Burn severity and vegetation recovery have been correlated in other systems (e.g., Pierce et al., 2004; Elena et al., 2019).

Together, poor vegetation recovery and moderate- to high-severity burn is associated with high sedimentation following larger precipitation events in our systems

in both 2015 and 2016, which is consistent with results from previous studies focused on post-wildfire sedimentation (e.g., Moody et al., 2001; Lane et al., 2006; Murphy et al., 2015). The South Fork basin maintained the strongest correlations between the total storm volume and turbidity responses to precipitation of all burned watersheds (2015: Pearson's R = 0.89, p-value = 0.003; 2016: Pearson's R = 0.84, p-value = 0.001) as well as peak I-10 precipitation intensity (Post-snowmelt 2015: Pearson's R = 0.74, p-value = 0.04), indicating that poor vegetation recovery and moderate- to high-severity burn is also associated with large turbidity responses triggered by high intensity precipitation. The South Fork basin, which experienced larger turbidity responses to storms from July-September than 2 of the 3 other burned watersheds in both 2015, was also the only watershed with a burned area with more than 50% south-facing (58%; Figure 2.3B). Consequently, the burned area in the South Fork basin may have experienced a smaller snowpack (e.g., Lopez-Moreno et al., 2014), which would result in the soil being exposed to precipitation earlier in the season than the other, more north-facing burned watersheds and therefore more susceptible to higher turbidity rates. All watersheds, burned and unburned, with the exception of Box Canyon, saw a decrease in average turbidity in 2016 from snowmelt (May-June) to post-snowmelt (July-September) (Figure 2.8C and Figure 2.8D; Table A.3). This shift in turbidity trend, where burned watersheds behaved more similarly to unburned watersheds in 2016, could be indicative of post-fire recovery in the burned watersheds. The summer of 2016 was the third summer following the WFC fire, which is when many burned watersheds have been found to exhibit turbidity and sedimentation trends similar to pre-fire conditions (Neary et al., 1998; Ryan et al., 2011; Hallema et al., 2017; Lucas-Borja et al., 2019). It is also possible that the sediment once mobilized from the burned hillslopes are now stored in the stream channels, remobilizing and increasing turbidity during larger discharge events, in which case vegetation cover on the hillslopes would not have as much of an effect on stream turbidity. This hypothesis fits with the turbidity-discharge relations in the South Fork, Thirty Mile, and Box Canyon watersheds (Figure 2.9), which showed that large increases in turbidity accompanied increases in discharge.

Lastly, we note that turbidity responses to precipitation are not always independently tied to singular events, and may be coerced by compounding environmental factors, such as historical climate or land-management practices (e.g., Turco et al., 2018). While our analysis looks to capture the effect existing watershed characteristics have on the sedimentation in burned watersheds following wildfire, effects from wildfire in our burned watersheds may exist beyond what is measured immediately following precipitation events, and may manifest itself further when coupled with future events, such as future wildfires, extreme rainfall, drought, or other climatic changes (Lima et al., 2017; Turco et al., 2018).

2.7 Conclusions

The current work looks to identify watershed characteristics associated with increased turbidity following wildfires, with the goal of predicting sedimentation as a function of slope aspect, soil type, slope, and vegetation distribution. In our seven watersheds, four of which were affected by the WFC fire in 2013, we note:

- Burned watersheds were not more prone to sedimentation than unburned watersheds during the spring snowmelt-driven runoff.
- Later in the summer, once snowmelt subsided, burned watersheds experienced higher average turbidity and larger turbidity responses to storms, indicating drivers of sedimentation in burned watersheds are more susceptible to precipitation than snowmelt.
- Watersheds with more soils that allow less infiltration in the burned area had larger turbidity responses to precipitation events than other watersheds.
- Strong vegetation recovery measured with EVI was not always associated with reduced turbidity response to storms, indicating other vegetation recovery metrics may be more useful in predicting sedimentation trends.
- Hillslopes may recover before channels, reducing the importance of vegetation recovery on predicting increases in turbidity as vegetation recover.
- The watershed with the highest burn severity and poorest vegetation recovery experienced the strongest positive correlations between total storm volume and turbidity response.

- Watershed slope as a single variable did not predict which watersheds would experience larger turbidity responses to precipitation events.

As has been seen at numerous other sites, burned watersheds experienced higher turbidity and larger turbidity responses to storms than unburned watersheds. At our site, this change only became apparent later in the summer once the snowmelt-driven spring runoff had subsided. Trends in turbidity responses to precipitation in burned watersheds later in the summer suggest that pre-fire soil properties are the watershed characteristic most able to predict the vulnerability of watersheds to severe sedimentation problems following wildfire. Our results also suggest that snow may act as an effective groundcover, reducing precipitation driven erosion in burned areas early in the spring. While vegetation recovery certainly plays a role in reducing sedimentation following wildfires, EVI was not the most effective metric for predicting how vegetation recovery would impact turbidity, indicating that canopy cover, which is captured well by EVI, may be less important for sedimentation reduction than hillslope armoring by roots and larger rock fragments. In the area of the WFC fire, we find that watersheds that experience frequent high-intensity precipitation and contain erosive soils, lower snowpacks, and vegetation that recovers slowly from fire should prepare for large increases in sedimentation associated with increased wildfire frequency and intensity in the coming decades.

CHAPTER 3
FUTURE WORK

This work identified how turbidity trends in burned watersheds differed from those in unburned watersheds following the 2013 West Fork Complex (WFC) fire in southeast Colorado throughout the summer, as well as how various characteristics of burned watersheds correlated to turbidity responses to precipitation. There are some limitations of this work, which I look to explore here as motivation for future work. Given the opportunity to continue this work, I would propose focusing on addressing four limitations of this study: vegetation characterization, estimating total suspended solids (TSS), geographic and ecological variety, and the number of unique watersheds included in the study.

Due to the geographic proximity of the seven studied watersheds to each other, it is possible that some watershed characteristics that control post-fire sedimentation were not variant enough between the seven watersheds to cause significant differences in our results. For example, soil types in the watersheds were classified based on gSSURGO's Hydrologic Soil Groups, which is a measure of the erosivity of soil. However, each of the seven watersheds lays in the San Juan Mountain range and is geologically similar, dominated by ash-flow deposits typical of the San Juan Mountains. While local variability in soil erosivity was observed, soil sourced from unique geological systems may react differently to wildfire in ways that were not captured in this study.

This project also looked at vegetation more through the lens of health and recovery than vegetation type. Aside from an observation that the Little Squaw basin contained a large population of aspen trees (*Pupulus tremuloides*) relative to the other watersheds, the distribution of vegetation types was not measured. Other studies have shown that other vegetation characteristics, such as vegetation type and density, play a role in how watersheds respond to precipitation (e.g., Kim et al., 2008); however EVI and EVI recovery were largely ineffective in predicting turbidity in our watersheds. To capture the role of vegetation in controlling sedimentation in watersheds post-wildfire, I would recommend conducting field surveys that characterized the vegetation type, density, root depth, and overall health of the vegetation in each watershed. These

surveys would provide nominal data, which could be analyzed in a corollary or multivariate framework to provide more detail as to what aspects of vegetation control sedimentation post-wildfire.

I would also recommend collecting more frequent TSS measurements as well as discharge in each of the watersheds. In this study, TSS was measured bi-weekly, which did not provide enough resolution to accurately relate TSS measurements to turbidity measurements. Turbidity has been shown to be linearly correlated to TSS, although specific relation coefficients between turbidity and TSS are dependent on geological and ecological factors of the contributing watershed (e.g., Rügner et al., 2014). By measuring TSS at a sub-daily frequency, concurrent turbidity and TSS concentrations would be captured at various levels of turbidity and TSS, allowing the calculation of the relation coefficient. Using turbidity to calculate instantaneous TSS concentrations and multiplying by the discharge rate of the stream, a total volume of sediment could be calculated for any period of time in each watershed. Although the geology in each of the seven studied watersheds was assumed to be relatively similar in our study, calculating the specific relation turbidity to TSS relation coefficient for each watershed individually could provide additional insight as to how small variations in watershed characteristics affect sedimentation rates and allow us to more accurately compare volumes of sediment leaving each watershed.

Finally, I would recommend repeating the same study in multiple locations. The WFC study area provided pairs of burned and unburned basins of similar size and geological characteristics, which was valuable for identifying how turbidity in watersheds responded to wildfire. However, due to the geographical proximity of the seven watersheds, there may not have been enough variation in watershed characteristics to associate differences in turbidity to specific watershed characteristics that have been shown to affect sedimentation, such as soil type, vegetation type, and precipitation regime. Increasing the number of watersheds with varying watershed characteristics and sedimentation trends following wildfire could also allow stronger multivariate analysis (see attempts in Appendix E). Our study was unsuccessful in performing multivariate linear regressions between the dependent variable, turbidity, and

independent variables, watershed characteristics, due to the limited number of watersheds and therefore variety in watershed characteristics. Multivariate regressions could provide insight into the potential compounding effects of multiple watershed characteristics on sedimentation. Similar studies analyzing sedimentation in multiple watersheds post-wildfire focusing on single-variable relationships have been done in Australia (Lane et al., 2006) and Canada (e.g., Silins et al., 2009); more studies using multivariate regression analysis were done in Colorado (e.g., de Dios Benavides-Solorio, 2003; Kunze et al., 2006), though all were performed with varying objectives and methods of data collection. By performing similar studies in multiple areas with different geological and ecological characteristics and comparing the total sediment volume leaving each watershed between study areas, we can continue to build a global database that can be used to help identify which watershed characteristics have the largest influence on sedimentation after wildfire in given systems.

REFERENCES

Al-Yaseri, I., Morgan, S., & Retzlaff, W. (2013). Using turbidity to determine total suspended solids in storm-water runoff from green roofs. *Journal of Environmental Engineering* (United States), 139(6), 822–828. https://doi.org/10.1061/(ASCE)EE.1943-7870.0000685

Bladon, K. D., Emelko, M. B., Silins, U., & Stone, M. (2014). Wildfire and the future of water supply. *Environmental Science and Technology,* 48(16), 8936–8943. https://doi.org/10.1021/es500130g

Chin, A., An, L., Florsheim, J. L., Laurencio, L. R., Marston, R. A., Solverson, A. P., Simon, G. L., Stinson, E., & Wohl, E. (2016). Geomorphology Investigating feedbacks in human – landscape systems: Lessons following a wildfire in Colorado, USA. *Geomorphology,* 252, 40–50. https://doi.org/10.1016/j.geomorph.2015.07.030

Cohen, J. (1988). Statistical power analysis for the behavioral sciences (2nd ed.). New York: Academic Press.

Crouch, R. L., Timmenga, H. J., Barber, T. R., & Fuchsman, P. C. (2006). Post-fire surface water quality: Comparison of fire retardant versus wildfire-related effects. *Chemosphere*, 62(6), 874–889. https://doi.org/10.1016/j.chemosphere.2005.05.031

de Dios Benavides-Solorio, J. (2003). Post-Fire Runoff and Erosion at the Plot and Hillslope Scale, Colorado Front Range. Colorado State University.

Debano, L. F. (2000). The role of fire and soil heating on water repellency in wildland environments: a review. *Journal of Hydrology*, 231-232, 195–206.

DiBiase, R. A., & Lamb, M. P. (2020). Dry sediment loading of headwater channels fuels post-wildfire debris flows in bedrock landscapes. *Geology*, 48(2), 189–193. https://doi.org/10.1130/G46847.1

Downing, J. (2006). Twenty-five years with OBS sensors: The good, the bad, and the ugly. *Continental Shelf Research*, 26, 2299–2318. https://doi.org/10.1016/j.csr.2006.07.018

Dunn, O. J. (1964). Multiple Comparisons using rank sums. *Technometrics*, 6, 241–252.

Ebel, B. A., Rengers, F. K., & Tucker, G. E. (2015). Aspect-dependent soil saturation and insight into debris-flow initiation during extreme rainfall in the Colorado Front Range. *Geological Society of America*, 43(8), 659–662. https://doi.org/10.1130/G36741.1

Elena, C., & Natalya, F. (2019). Monitoring of Post-Fire Burn Severity and Vegetation. *Section Geoimformatics*, 965–973.

Erickson, T. A., Williams, M. W., & Winstral, A. (2005). Persistence of topographic controls on the spatial distribution of snow in rugged mountain terrain, Colorado, United States. *Water Resources Research*, 41(4), 1–17. https://doi.org/10.1029/2003WR002973

Fan, J., & Morris, G. L. (1992). Reservoir Sedimentation. I: Delta and Density Current Deposits. *Journal of Hydraulic Engineering,* 118(3), 354–369.

Garen, D. C. (1993). Revised Surface-Water Supply Index for Western United States. *Journal of Water Resources Planning and Management,* 119(4), 437–454.

Godsey, S. E., Kirchner, J. W. and Clow, D. W. (2009). Concentration-discharge relationships reflect chemostatic characteristics of US catchments. *Hydrological Processes*, 23, pp. 1844–1864. https://doi.org/10.1002/hyp.7315

Graham, R. T. (2003). Hayman Fire Case Study. General Technical Report RMRS-GTR-114. Rocky Mountain Research Station, Forest Service, United States Department of Agriculture.

Hallema, D. W., Sun, G., Bladon, K. D., Norman, S. P., Caldwell, P. V., Liu, Y., & McNulty, S. G. (2017). Regional patterns of post-wildfire streamflow response in the Western United States: The importance of scale-specific connectivity. *Hydrological Processes*, 31(14), 2582–2598. https://doi.org/10.1002/hyp.11208

Hassan, M. A., Church, M., Lisle, T. E., Brardinoni, F., Benda, L., & Grant, G. E. (2005). Sediment transport and channel morphology of small, forested streams. *Journal of the American Water Resources Association*, 41(4), 853–876. https://doi.org/10.1111/j.1752-1688.2005.tb03774.x

Hohner, A. K., Cawley, K., Oropeza, J., Summers, R. S., & Rosario-Ortiz, F. L. (2016). Drinking water treatment response following a Colorado wildfire. *Water Research*, 105, 187–198. https://doi.org/10.1016/j.watres.2016.08.034

Hollander, M., & Wolfe, D. (1973). Nonparametric Statistical Methods. New York: John Wiley & Sons.

Hunsaker, C. T. and Johnson, D. W. (2017). Concentration-discharge relationships in headwater streams of the Sierra Nevada, California. *Water Resources Research*, 53(9), pp. 7869–7884. doi: 10.1002/2016WR019693

Jarchow, C. J., Didan, K., Barreto-muñoz, A., Nagler, P. L., & Glenn, E. P. (2018). Enhanced Vegetation Index to VIIRS, Landsat 5 TM and Landsat 8 OLI Platforms: A Case Study in the Arid Colorado River Delta, Mexico. *Sensors*, (18). https://doi.org/10.3390/s18051546

Jones, K. W., Cannon, J. B., Saavedra, F. A., Kampf, S. K., Addington, R. N., Cheng, A. S., MacDonald, L. H., Wilson, C., & Wolk, B. (2017). Return on investment from fuel treatments to reduce severe wildfire and erosion in a watershed investment program in Colorado. *Journal of Environmental Management*, 198, 66–77. https://doi.org/10.1016/j.jenvman.2017.05.023

Kalra, A., & Ahmad, S. (2011). Evaluating changes and estimating seasonal precipitation for the Colorado River Basin using a stochastic nonparametric disaggregation technique. *Water Resources Research*, 47(5), 1–26. https://doi.org/10.1029/2010WR009118

Keeley, J.E. (2009). Fire intensity, fire severity, and burn severity: a brief review and suggested usage. *International Journal of Wildland Fire*, 18(1), 116-126.

Kim, C. G., Shin, K., Joo, K. Y., Lee, K. S., Shin, S. S., & Choung, Y. (2008). Effects of soil conservation measures in a partially vegetated area after forest fires. *Science of the Total Environment*, 399(1–3), 158–164. https://doi.org/10.1016/j.scitotenv.2008.03.034

Kunze, M. D., & Stednick, J. D. (2006). Streamflow and suspended sediment yield following the 2000 Bobcat fire, Colorado. *Hydrological Processes*, 1681(March 2005), 1661–1681. https://doi.org/10.1002/hyp.5954

Lane, P., Sheridan, G., & Noske, P. (2006). Changes in sediment loads and discharge from small mountain catchments following wildfire in south eastern Australia. *Journal of Hydrology*, 331(3–4), 495–510. https://doi.org/10.1016/j.jhydrol.2006.05.035

Lima, C. H. R., Aghakouchak, A., & Randerson, J. (2017). Unraveling the Role of Temperature and Rainfall on Active Fires in the Brazilian Amazon Using a Nonlinear Poisson Model*. AGU Publications*. https://doi.org/10.1002/2017JG003836

Loomis, J., Sánchez, J. J., González-Cabán, A., Rideout, D., & Reich, R. (2018). Do Fuel Treatments in U.S. National Forests Reduce Wildfire Suppression Costs and Property Damages? *Journal of Natural Resources Policy Research*. https://doi.org/10.5325/naturesopolirese.9.1.0042

Lopez-Moreno, J. I., Revuelto, J., Gilaberte, M., Moran-Tejeda, E., Pons, M., Jover, E., Esteban, P., García, C., & Pomeroy, J. W. (2014). The effect of slope aspect on the response of snowpack to climate warming in the Pyrenees. *Theoretical and Applied Climatology*, 207–219. https://doi.org/10.1007/s00704-013-0991-0

Lucas-Borja, M. E., González-Romero, J., Plaza-Álvarez, P. A., Sagra, J., Gómez, M. E., Moya, D., Gómez, M. E., & de las Heras, J. (2019). The impact of straw mulching and salvage logging on post-fire runoff and soil erosion generation under Mediterranean climate conditions. *Science of the Total Environment*, 654, 441–451. https://doi.org/10.1016/j.scitotenv.2018.11.161

Lyon, J. P. and O'Connor, J. P. (2008). Smoke on the water: Can riverine fish populations recover following a catastrophic fire-related sediment slug?. *Austral Ecology*, 33(6), pp. 794–806. doi: 10.1111/j.1442-9993.2008.01851.x

Martin, D. A. (2016). At the nexus of fire, water and society. *Philosophical Transactions of the Royal Society B: Biological Sciences*, 371(1696). https://doi.org/10.1098/rstb.2015.0172

Meyer, J. P. (2019). Hayman are still mucking up water. The Denver Post, 1–6. Retrieved from https://www.denverpost.com/2006/11/23/hayman-fire-still-mucking-up-water/

Miller, J. D., & Quayle, B. (2015). Calibration and Validation of Immediate Post-Fire Satellite-Derived Data to Three Severity Metrics. *Fire Ecology*, 11(2), 12–30. https://doi.org/10.4996/fireecology.1102012

Miller, J. D., & Yool, S. R. (2002). Mapping forest post-fire canopy consumption in several overstory types using multi-temporal Landsat TM and ETM data. *Remote Sensing of Environment*, 82, 481–496. https://doi.org/https://doi.org/10.1016/S0034-4257(02)00071-8

Miller, M. E., MacDonald, L. H., Robichaud, P. R., & Elliot, W. J. (2011). Predicting post-fire hillslope erosion in forest lands of the western United States. *International Journal of Wildland Fire*, 20(8), 982–999. https://doi.org/10.1071/WF09142

MODIS. (2020). About Data Tools Science Team Images News Related Sites MODARCH MODIS Vegetation Index Products (NDVI and EVI) About Data Tools Science Team Images News Related Sites. Retrieved from https://modis.gsfc.nasa.gov/data/dataprod/mod13.php

Moody, J. A., & Martin, D. A. (2001). Initial hydrologic and geomorphic response following a wildfire in the Colorado front range. *Earth Surface Processes and Landforms*, 26(10), 1049–1070. https://doi.org/10.1002/esp.253

Moody, J. A., Shakesby, R. A., Robichaud, P. R., Cannon, S. H., & Martin, D. A. (2013). Current research issues related to post-wildfire runoff and erosion processes. *Earth-Science Reviews*, 122, 10–37. https://doi.org/10.1016/j.earscirev.2013.03.004

Moritz, M. A., Batllori, E., Bradstock, R. A., Gill, A. M., Handmer, J., Hessburg, P. F., Leonard, J., McCaffrey, S., Odion, D. C., Schoennagel, T., & Syphard, A. D. (2014). Learning to coexist with wildfire. *Nature*, 515(7525), 58–66. https://doi.org/10.1038/nature13946

MTBS. (2020). MTBS Glossary. Retrieved from https://www.mtbs.gov/glossary

Murphy, S. F., Writer, J. H., McCleskey, R. B., & Martin, D. A. (2015). The role of precipitation type, intensity, and spatial distribution in source water quality after wildfire. *Environmental Research Letters*, 10(8). https://doi.org/10.1088/1748-9326/10/8/084007

Neary, D. G., Gottfried, G. J., & Ffolliott, P. F. (1998). Post-Wildfire Flood Responses. 1–8.

Niu, R. qing, Du, B., Wang, Y., Zhang, L. pei, & Chen, T. (2014). Impact of fractional vegetation cover change on soil erosion in Miyun reservoir basin, China. *Environmental Earth Sciences*, 72(8), 2741–2749. https://doi.org/10.1007/s12665-014-3179-8

Perreault, L. M., Yager, E. M., & Aalto, R. (2017). Effects of gradient, distance, curvature and aspect on steep burned and unburned hillslope soil erosion and deposition. *Earth Surface Processes and Landforms*, 42(7), 1033–1048. https://doi.org/10.1002/esp.4067

Pierce, J. L., Meyer, G. A., & Jull, A. J. T. (2004). Fire-induced erosion and millennial scale climate change in northern ponderosa pine forests. *Nature*, 432(November), 87–90. https://doi.org/10.1038/nature03028.Published

Pierson, F. B., Robichaud, P. R., Moffet, C. A., Spaeth, K. E., Hardegree, S. P., Clark, P. E., & Williams, J. C. (2007). Fire effects on rangeland hydrology and erosion in a steep sagebrush-dominated landscape. *Hydrological Processes*, 22, 2916–2929. https://doi.org/10.1002/hyp

Pierson, F. B., Williams, C. J., & Robichaud, P. R. (2015). Assessing impacts of fire and post-fire mitigation on runoff and erosion from rangelands. (Great Basin Factsheet Series, Number 11), 1–6.

Rahmani, V., Id, J. H. K., Jakubauskas, M. E., Martinko, E. A., Huggins, D. H., Gnau, C., Liechti, P. M., Campbell, S. W., Callihan, R. A., & Blackwood, A. J. (2018). Examining Storage Capacity Loss and Sedimentation Great Plains. *Water*, 1–17. https://doi.org/10.3390/w10020190

Robinne, F., Hallema, D. W., Bladon, K. D., Flannigan, M. D., Boisrame, G., Brethaut, C. M., Baldassarre, G. D., Louise, G., Hohner, A., Khan, S., Kinoshita, A. M., Martin, D., Mordecai, R., Nunes, J. P., Nyman, P., Santin, C., Sheridan, G., Stoof, C., Thompson, M. P., Waddington, J. M., Wei, Y. (2021). Short running title: Warning on wildfire and water supply. https://doi.org/10.1002/hyp.14086

Rügner, H., Schwientek, M., Beckingham, B., Kuch, B., & Grathwohl, P. (2013). Turbidity as a proxy for total suspended solids (TSS) and particle facilitated pollutant transport in catchments. *Environmental Earth Sciences,* 69(2), 373–380. https://doi.org/10.1007/s12665-013-2307-1

Rügner, H., Schwientek, M., Egner, M., & Grathwohl, P. (2014). Monitoring of event-based mobilization of hydrophobic pollutants in rivers: Calibration of turbidity as a proxy for particle

facilitated transport in field and laboratory. *Science of the Total Environment*, 490, 191–198. https://doi.org/10.1016/j.scitotenv.2014.04.110

Rust, A. J. (2017). Wildfire in the West: Evaluating Water Quality and Ecosystem Impacts and Their Controlling Factors. Colorado School of Mines.

Rust, A. J., Hogue, T. S., Saxe, S., & McCray, J. (2018). Post-fire water-quality response in the western United States. *International Journal of Wildland Fire*, 27(3), 203–216.

Rust, A. J., Randell, J., Todd, A. S., & Hogue, T. S. (2019). Wildfire impacts on water quality, macroinvertebrate, and trout populations in the Upper Rio Grande. *Forest Ecology and Management*, 453(February), 117636. https://doi.org/10.1016/j.foreco.2019.117636

Ryan, S. E., Dwire, K. A., & Dixon, M. K. (2011). Impacts of wildfire on runoff and sediment loads at Little Granite Creek, western Wyoming. *Geomorphology*, 129(1–2), 113–130. https://doi.org/10.1016/j.geomorph.2011.01.017

Sankey, J. B., Kreitler, J., Hawbaker, T. J., McVay, J. L., Miller, M. E., Mueller, E. R., Vaillant, N. M., Lowe, S. E., & Sankey, T. T. (2017). Climate, wildfire, and erosion ensemble foretells more sediment in western USA watersheds. *Geophysical Research Letters*, 44(17), 8884–8892. https://doi.org/10.1002/2017GL073979

Schroder, E. (2013). West Fork Complex BAER Report. Reference: FSH 2509.13. USDA-Forest Service.

Silins, U., Stone, M., Emelko, M. B., & Bladon, K. D. (2009). Sediment production following severe wildfire and post-fire salvage logging in the Rocky Mountain headwaters of the Oldman River Basin, Alberta. *Catena*, 79(3), 189–197. https://doi.org/10.1016/j.catena.2009.04.001

Smith, J. (2021). No blarney : State approves up to $75 million for water projects, fire-scarred watersheds, *Water Education Colorado*, March, pp. 1–5. Available at: https://www.watereducationcolorado.org/fresh-water-news/no-blarney-state-authorizes-up-to-75-million-for-water-projects-fire-scarred-watersheds/.

Smith, H. G., Sheridan, G. J., Lane, P. J., Nyman, P., & Haydon, S. (2011). Wildfire effects on water quality in forest catchments: A review with implications for water supply. *Journal of Hydrology*, 396(1–2), 170–192. https://doi.org/10.1016/j.jhydrol.2010.10.043

Stottlemyer, R., Troendle, C. A., & Markowitz, D. (1997). Change in snowpack, soil water, and streamwater chemistry with elevation during 1990, Fraser Experimental Forest, Colorado. *Journal of Hydrology,* 195(1–4), 114–136. https://doi.org/10.1016/S0022-1694(96)03241-6

Tran, B. N., Tanase, M. A., Bennett, L. T., & Aponte, C. (2018). Evaluation of spectral indices for assessing fire severity in Australian temperate forests. *Remote Sensing*, 10(11), 1–18. https://doi.org/10.3390/rs10111680

Turco, M., Jerez, S., Doblas-reyes, F. J., Aghakouchak, A., Llasat, M. C., & Provenzale, A. (2018). Skillful forecasting of global fire activity using seasonal climate predictions. *Nature Communications*. https://doi.org/10.1038/s41467-018-05250-0

USDA-ARS National Soil Erosion Research Laboratory. (2017). Water Erosion Prediction Project (WEPP). Retrieved from https://data.nal.usda.gov/dataset/water-erosion-prediction-project-wepp

Valentin, M. M. (2017). Identifying Climate-Related Hydrologic Regime Changes in Mountainous, Cold-Region Watersheds (Colorado School of Mines). Retrieved from http://library1.nida.ac.th/termpaper6/sd/2554/19755.pdf

Wall, S. A., Roering, J. J., & Rengers, F. K. (2020). Runoff-initiated post-fire debris flow Western Cascades, Oregon. *Landslides*, (October 2019), 1649–1661. https://doi.org/10.1007/s10346-020-01376-9

Westerling, A. L., Hidalgo, H. G., Cayan, D. R., & Swetnam, T. W. (2006). Warming and earlier spring increase Western U.S. forest wildfire activity. *Science*, 313(5789), 940–943. https://doi.org/10.1126/science.1128834

Wilson, C., Kampf, S. K., Wagenbrenner, J. W., & Macdonald, L. H. (2018). Forest Ecology and Management Rainfall thresholds for post-fire runoff and sediment delivery from plot to watershed scales. *Forest Ecology and Management*, 430(November 2017), 346–356. https://doi.org/10.1016/j.foreco.2018.08.025

Yochum, S. E. & Norman, J. B. (2014). West Fork Complex Fire: Potential Increase in Flooding and Erosion. U. S. Department of Agriculture, Natural Resources Conservation Service, Colorado, 32 Pages, (101185). https://doi.org/10.13140/2.1.4165.8887

APPENDIX A

SUPPLEMENTAL MATERIAL FOR THE MANUSCRIPT

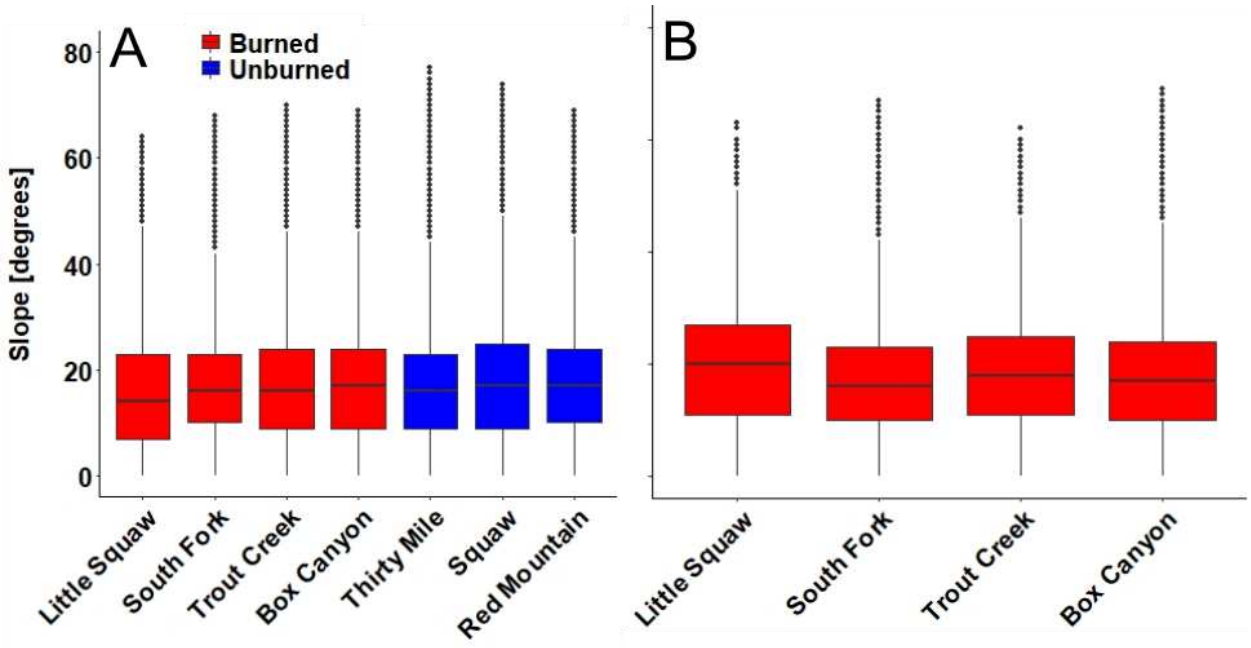

Figure A.1: Distributions of slope measured at a 10m resolution over (A) the entire watershed and (B) inside the burned perimeter of the burned watersheds. The Squaw basin had the highest average slope (A) compared to all other watersheds. The South Fork basin inside the burn perimeter had the lowest average slope (B) compared to the other burned areas.

Table A.1: Average storm volume and total precipitation received in each watershed from May-September of 2015 and 2015. Box Canyon shared a precipitation gage with Thirty Mile, Squaw shared a precipitation gage with Little Squaw, Trout Creek shared a precipitation gage with Red Mountain, and South Fork had its own precipitation gage. Precipitation events producing more than 5mm of precipitation were considered storms. Total precipitation includes all precipitation received throughout the season, not just from identified storms.

	2015			2016		
Watersheds	# Storms	Median Storm Volume (mm)	Total May - Sep Precipitation Received (mm)	# Storms	Median Storm Volume (mm)	Total May - Sep Precipitation Received (mm)
Box Canyon / Thirty Mile	14	7.4	206.0	15	8.1	254.5
Squaw / Little Squaw	17	14.2	339.3	21	8.6	312.2
Trout Creek / Red Mountain	19	10.9	349.3	11	11.9	271.5
South Fork	12	8.3	173.2	17	7.1	259.3

Table A.2: Number of storms that triggered a turbidity response larger than 33% of the weekly median turbidity measurement compared to the number of storms identified in each watershed. Fewer storms triggered a turbidity response across all watersheds in 2016 than 2015. Paired basins shared precipitation gage: SG01 - Box Canyon and Thirty Mile, RG05 – Squaw/Little Squaw, RG02 – Trout Creek/Red Mountain, RG01 – South Fork. Due to gaps in turbidity data, some watersheds have fewer storms with a measurable turbidity response than their paired basin.

		2015		2016	
# Storm Responses / # Storms	Burned?	May-Jun	Jul-Sept	May-Jun	Jul-Sept
Box Canyon	Y	3/3	8/10	2/4	2/12
Thirty Mile	N	0/3	3/7	0/4	4/10
Squaw	N	5/5	6/11	2/5	2/14
Little Squaw	Y	5/5	10/10	5/5	13/17
Trout Creek	Y	5/6	10/12	0/2	0/6
Red Mountain	N	2/2	12/12	0/4	2/7
South Fork	Y	0/0	8/8	0/5	5/12

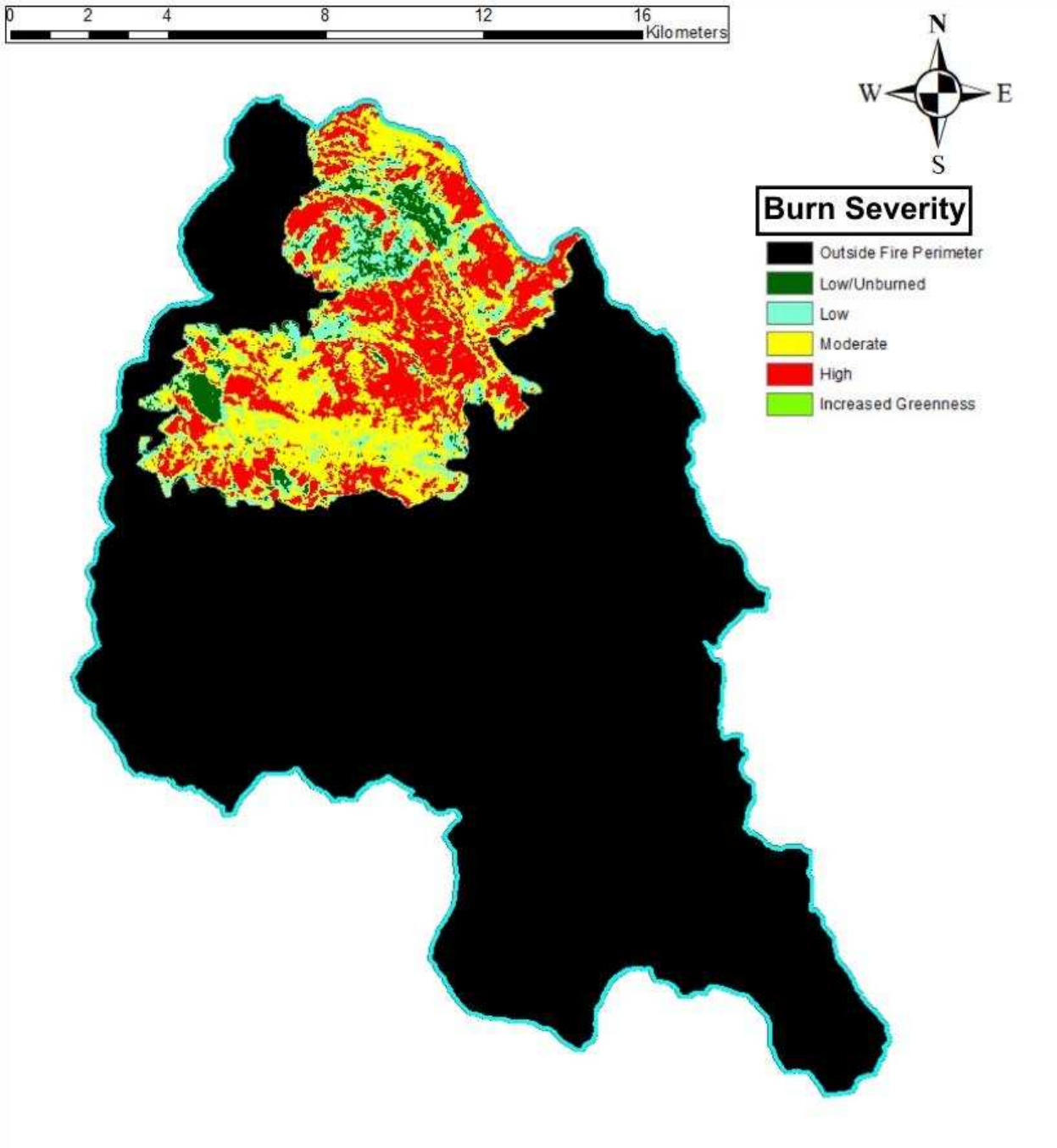

Figure A.2: Monitoring Trends in Burn Severity (MTBS) 30-m Thematic Burn Severity layer in the South Fork basin. The Thematic Burn Severity layer used to classify the percentage of each of the four burned watersheds burned at a low, moderate, or high severity.

Table A.3: Average turbidity measurements during runoff (May - June) and post-runoff (July - September) of 2015 and 2016. Turbidity was higher in 2016 than 2015 for most watersheds. Burned watersheds often experienced higher mean turbidity measurements post-runoff, while turbidity in unburned watersheds always decreased from runoff to post-runoff. The standard deviation of turbidity measurements in burned watersheds was often higher than the standard deviation calculated in their paired unburned watershed, especially post-runoff. *Turbidity data in South Fork was only collected through August of 2015.

Watershed	Burned?	Mean (NTUs)	SDV (NTUs)	Mean (NTUs)	SDV (NTUs)
2015		May-June		July-September	
Box Canyon	Y	145	509	292	821
Thirty Mile	N	18	52	7	32
Squaw	N	24	171	0	3
Little Squaw	Y	11	41	15	159
Trout Creek	Y	43	197	3	5
Red Mountain	N	209	712	2	3
South Fork*	Y	10	12	31	213
2016		May-June		July-September	
Box Canyon	Y	540	799	795	1184
Thirty Mile	N	265	139	253	715
Squaw	N	36	152	7	65

Table A.3 Continued

Little Squaw	Y	29	20	27	21
Trout Creek**	Y	2032	1347	1689	1408
Red Mountain	N	524	853	1	19
South Fork	Y	32	34	7	26

Qualitative Comparison of Turbidity Responses to Storms

The differences in turbidity response to precipitation events between burned and unburned watersheds was more apparent post-runoff (July - September) than during runoff (May - June) in both 2015 and 2016. As was apparent in the average turbidity measurements during runoff and post-runoff (Figure 2.8) and the turbidity response measurements (Figure 2.11), fluctuations in turbidity surrounding storms were similar between paired basins early in the season (May - June) and different between paired basins later in the season (July - September). During runoff, paired basins Squaw (unburned) and Little Squaw (burned) experience diurnal fluctuations in turbidity before the storm arrives (Figure A.3). In the hours following the storm, both watersheds experienced similarly elevated turbidity before lowering back to pre-storm levels (Figure A.3). After runoff, in mid-July, both watersheds experience baseline turbidity near 0 NTUs before the storm arrives (Figure A.3). After the storm arrived, elevated turbidity was much more apparent in Little Squaw, the burned watershed, than Squaw, the unburned watershed (Figure A.3). Turbidity in Squaw was only elevated above its baseline turbidity of 0 NTUs for a few hours, and at a much lower magnitude than Little Squaw's turbidity response, while Little Squaw continued to react to each precipitation event, regardless of size.

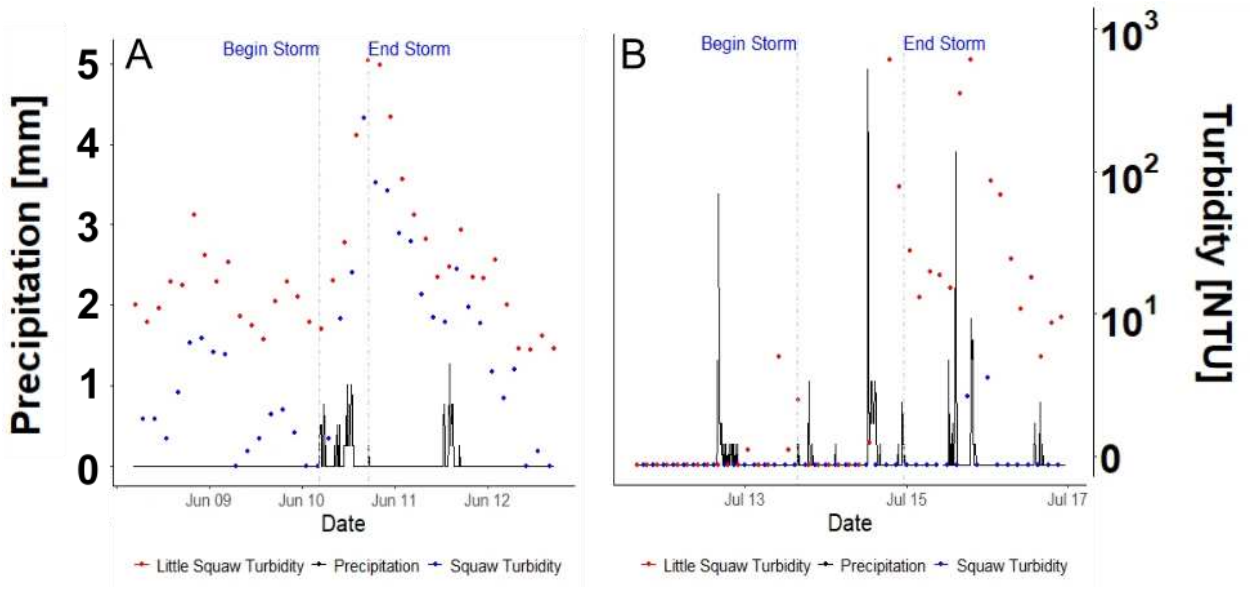

Figure A.3: Precipitation and turbidity measurements in paired basins Squaw (unburned) and Little Squaw (burned) during (A) June and (B) July of 2015. Precipitation was measured at ten-minute intervals, while turbidity was measured at three-hour intervals. Turbidity was log-transformed due to large swings in turbidity following storms. Turbidity is non-zero and fluctuating before the storm (A) during runoff for both watersheds, and both watersheds react with similar amplitude to the storms. (B) Post-runoff, turbidity is near zero for both watersheds before the storm, but Little Squaw's turbidity response to the storm is much more apparent than its unburned paired watershed, Squaw.

Table A.4: Regression slopes, standard error of slope, and r^2 values for linear regressions calculated between log-turbidity and log-discharge in the South Fork, Thirty Mile, and Box Canyon watersheds during peak snowmelt (May-June), post-snowmelt (July-September), and the entire season (May-September). South Fork and Box Canyon were burned watersheds, Thirty Mile was unburned.

2015				
Watershed	Snowmelt (May-June)		Post-Snowmelt (July-September)	
	Slope	r^2	Slope	r^2
South Fork	0.41 ± 0.01	0.19	1.63 ± 0.02	0.44
Thirty Mile	0.82 ± 0.01	0.47	0.67± 0.02	0.20
Box Canyon	2.27 ± 0.03	0.49	-0.04 ± 0.03	0.00
2016				
	Slope	r^2	Slope	r^2
South Fork	2.07 ± 0.02	0.64	-0.50 ± 0.04	0.02
Thirty Mile	1.79 ± 0.14	0.03	-0.49 ± 0.06	0.01
Box Canyon	-0.56 ± 0.14	0.00	2.04 ± 0.10	0.05
All (May-September)				
	2015		2016	
	Slope	r^2	Slope	r^2
South Fork	0.94 ± 0.01	0.51	0.90 ± 0.01	0.37
Thirty Mile	0.85 ± 0.01	0.40	1.68± 0.02	0.27
Box Canyon	-0.10 ± 0.02	0.00	0.90 ± 0.03	0.06

APPENDIX B

ESTIMATING TSS USING TURBIDITY

In an attempt to compare sedimentation between watersheds, a relation between turbidity and discharge was used to estimate the volume of sediment leaving each watershed. Because discharge was not recorded in the smaller tributaries, watershed area and mean annual discharge relations were used to estimate discharge in each watershed based on discharge data collected in the South Fork basin. A specific turbidity to TSS relation coefficient is also needed to estimate sediment loads based on turbidity, which was not possible to calculate due to the small number of TSS samples taken in each watershed throughout the study period. Therefore, the TSS to turbidity relation coefficient was estimated to be the same for each watershed. Because discharge was so similar for each watershed and a unique turbidity to TSS was not able to be calculated, little variation in sediment loads was seen between watersheds. In addition to a lack of results, a large amount of uncertainty was built into the sediment load volumes due to compounding estimates. Because of the potential for error and lack of results, turbidity alone was used to compare sedimentation without citing specific volumes of sediment.

Turbidity data were used to estimate relative sediment loads leaving each of the seven watersheds. Turbidity data for each watershed was statistically re-sampled to have comparable hourly temporal resolution using linear interpolation built into the MATLAB *retime* function from May 7, 2015 to August 28, 2015 and May 16, 2016 to October 1, 2016; these two periods are the summertime periods during which all five watersheds were recording turbidity data and the South Fork gage was also recording discharge data. To compare relative sediment loads between watersheds instead of sediment concentrations, we converted our turbidity data into total sediment yield. Because the relation between TSS and turbidity is geology dependent (Downing, 2006), determining the actual volume of sediment accompanying turbidity measurements requires sampling of both TSS and turbidity and determining a model between the two for every unique watershed. During the time period which turbidity data for this project was collected, TSS was only sampled on a bi-weekly basis, which did not

provide enough data points to calibrate the relation between NTUs and TSS concentrations in our watersheds. However, because of the selected watersheds' similar geology and relative geographic proximity to one another, the relation coefficient between turbidity and TSS concentrations should be the same for all five of the watersheds (Downing, 2006; Rügner et al., 2013). Therefore, each watershed's TSS concentration would be estimated by multiplying its turbidity measurements by the same coefficient were it known (Rügner et al., 2013). Using turbidity values in NTU as a TSS concentration value, effectively setting the unknown TSS to NTU relation coefficient to one, allows us to quantitatively compare sediment loads between the five watersheds using these unitless TSS concentrations. Calculating actual sediment yield using turbidity measurements is impossible without the unique TSS to NTU coefficient, but relative sediment yields between these five basins will remain the same regardless of the coefficient used. To convert TSS concentrations into total sediment yield for a given watershed, the TSS concentration is multiplied by the discharge rate of the stream.

Estimating Discharge

Discharge data were only collected for the South Fork basin during this study; to estimate discharge in the four remaining basins, the discharge recorded in the South Fork basin was scaled for each remaining watershed by relative area. The relation between contributing watershed area and discharge volume in watersheds across the United States has been described as:

$$Q = k \cdot A^c$$

where Q is discharge in m^3/s , k is a unitless discharge coefficient, A is the area in km^2 of the watershed contributing to the point of interest in the stream, and c is the exponential relation coefficient between area and stream discharge (e.g., Whipple, 2004). In humid coastal climates, the discharge-to-area exponential relation coefficient c is close to one, indicating a linear correlation between watershed area and stream discharge (Whipple, 2004; Cragun, 2005; Gianfagna et al., 2015). More arid regions, such as the Colorado Plateau, show lower and more variable exponential relation

coefficients than more humid coastal environments (Cragun, 2005; Galster et al., 2006; Galster, 2007).

Cragun (2005) identified regional relations between drainage area and stream discharge on the Colorado Plateau. Drainages in the northern portion of the Colorado Plateau showed an exponential relation coefficient of ~0.7, whereas drainages in the southern portion showed an exponential relation coefficient of ~0.65. The northern drainages grouping identified by Cragun include major drainages in the Gunnison, Upper Colorado, and San Juan basins. Because the WFC study area lies in the San Juan Mountain range near the headwaters to the San Juan river basin, they should have similar geology and aridity, two major factors affecting the drainage area to discharge relation (Whipple, 2004; Galster, 2007). Therefore, the drainage area to discharge relation for the WFC study area should be similar to those in the northern drainage groupings. Consequently, the mean annual discharge in our four ungauged watersheds was estimated using the model for Northern Drainages presented by Cragun (2005), where the mean annual discharge $Q_{mean} = 0.0803 \cdot A^{0.7}$ in m^3/s. This relation provided a mean annual discharge of 146 m^3/s in the South Fork basin. The mean discharge measured in the South Fork basin from May through September was 153 m^3/s for both 2015 and 2016. The mean annual baseflow for the South Fork basin is likely much smaller than this when including lower winter baseflows. While this may indicate that the Cragun relation overestimates mean annual discharge in the WFC study area, it does provide a reasonable estimate of relative discharge during the study period (Table B.1)

Table B.1: Estimated Mean Annual Discharge from Cragun (2005) relation

Watershed	**Area (km^2)**	**Mean Annual Discharge (m^3/s)**	**Fraction of South Fork Discharge**
Squaw	89	1.9	0.45
Little Squaw	74	1.6	0.39
Trout Creek	34	1.0	0.23
Red Mountain	131	2.4	0.59
South Fork	279	4.1	1.00

Because of the geographic proximity between the basins in the WFC study area, it was assumed that discharge patterns would be similar between each of the basins, varying primarily by volume rather than timing. Discharge was recorded in the South Fork basin through the summers of 2015 and 2016 at 15-minute intervals, and was re-sampled in MATLAB using linear interpolation in the built in *retime* function to match turbidity measurement times. Hourly discharge was estimated for each basin by multiplying the hourly measurements from the South Fork basin by the fraction of mean annual discharge estimated for each respective basin to the estimated mean annual discharge from South Fork basin.

Estimating Sediment Yield

Turbidity in NTUs was multiplied by the discharge in m^3/s at each time step to get a relative volume of TSS (unitless) passing through the outflow of the watersheds each hour. Maintaining the hourly temporal resolution when multiplying turbidity and flow was imperative to capturing the larger fluxes of TSS resulting from high turbidity events coinciding with high flow events. Using mean annual flows to convert turbidity (or TSS

concentrations) into the volume of TSS loads for each watershed would have missed the large peaks in turbidity coinciding with large peaks in discharge, which increase the total volume of TSS more than turbidity or discharge on their own.

The larger watersheds, as expected, showed larger total amounts of TSS exiting the watershed throughout every period analyzed. To normalize TSS loads from watersheds of different size so that the relative TSS load as controlled by other watershed properties can be explored, total TSS volumes were divided by the total estimated discharge volume to create a normalized average TSS concentration for each watershed over every time period of interest:

$$TSS_{norm} = \frac{\sum_{hourly} Turbidity \cdot Q}{\sum_{hourly} Q}$$

where TSS_{norm} is the unitless TSS concentration normalized for watershed area. This averaged TSS concentration allowed comparison between watersheds of different size while still accounting the effect of varying turbidity accompanied by varying discharge. Normalized TSS concentrations were computed for weekly periods coinciding with 8-day average EVI values and annual field season periods coinciding with turbidity measurements to identify the effect of both temporally variant and static watershed characteristics have on TSS loads in all watersheds (Table B.1).

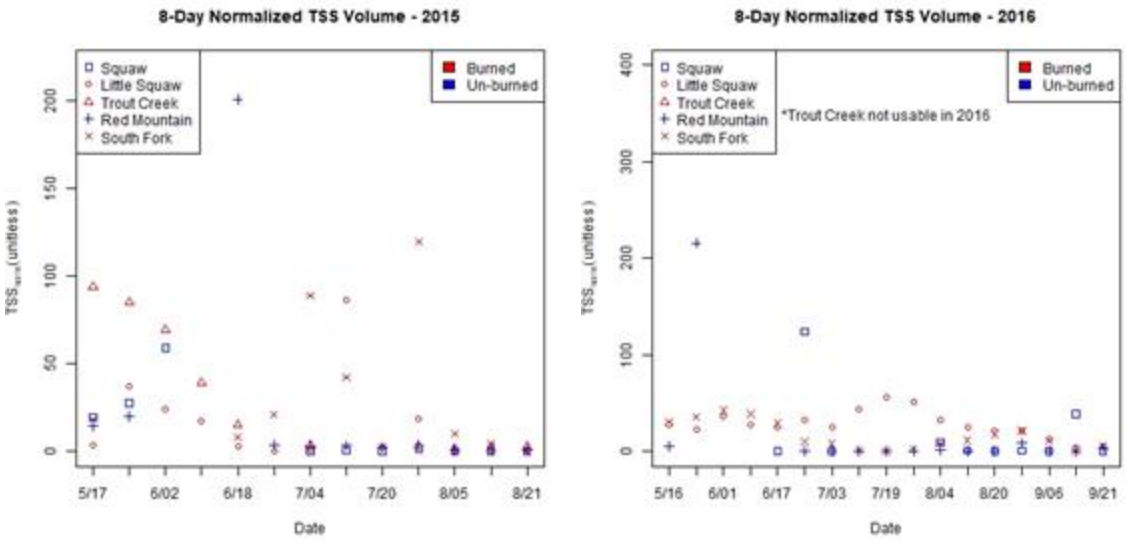

Figure B.1: Total TSS volume normalized for total discharge (TSS_{norm}) passing through each watershed during each 8-day period in 2015 and 2016. Burned watersheds generally experienced higher TSS_{norm} loads than unburned watersheds, although unburned watersheds also saw large pulses of TSS_{norm}, especially during spring runoff.

There were no apparent differences between the sediment loads leaving burned and unburned watersheds. In 2015, Little Squaw and Trout Creek exhibited sedimentation trends that showed higher sedimentation during runoff than later summer, while Little Squaw and South Fork followed similar trends in 2016 (Figure B.1). Aside from these three watersheds whose sedimentation rates mimicked discharge rates, there were also few discernible trends in estimated sediment loads throughout the summers of 2015 and 2016 (Figure B.1). One reason for the similarity in sedimentation rates between burned and unburned watersheds may be the lack of resolution; sedimentation volumes were only estimated for eight-day periods. This may not allow short but large sedimentation events, such as after a precipitation event, to appear when diluted by the lower baseline sedimentation happening the rest of the 8-day period. There are also a large number of assumptions and approximations built into the total sedimentation estimate, many of which are based on the same original dataset. For example, discharge estimates, which were a large part of the sediment estimation, were scaled linearly for each watershed based on total watershed area. This could cause sedimentation rates between watersheds to follow similar trends. Relation

coefficients between turbidity and TSS were also assumed to be the same for each watershed despite the coefficient's dependence on geological characteristics of the watersheds. This assumption also does not allow differences in watershed characteristics that play into the relation coefficient between turbidity and TSS to be fully explored, as the assumption that characteristics were identical has already been used. Because of the assumptions and estimates built in to the TSS calculations, we have less confidence in the dependent variable TSS_{norm} than in turbidity, which was measured directly. Turbidity, while not a direct measure of sedimentation, is linearly related to TSS concentrations (e.g., Rügner et al., 2013), and therefore can be used to assess changes in sedimentation rates. To reduce error and uncertainty in our results, we chose to move forward with using turbidity as the dependent variable.

APPENDIX C

ANALYZING TRENDS IN EVI OVER TIME

The mean and maximum EVI pixel value for each watershed was calculated for each available 8-day time frame for all time coinciding with turbidity, discharge, and precipitation collection times, creating 33 unique snapshots to compare the effects of temporally variant watershed characteristics on sedimentation in each of the seven watersheds. The 8-day mean EVI values for all seven watersheds follow similar trends throughout the seasons in 2015 and 2016, rising through the spring and early summer and falling towards the end of summer (Figure C.1). The rising limb of the average EVI plots for both 2015 and 2016, from May to early-July, the watersheds with the highest mean EVI are Trout Creek and South Fork, both burned watersheds. From mid-July through the end of the summer, Squaw, which is an unburned watershed, appears to have the highest mean EVI in both 2015 and 2016. Maximum EVI measurements follow a similar trend to mean EVI in both 2015 in 2016, but with less variation throughout the year. The highest maximum EVI values belonged to burned watersheds throughout almost the entire 2015 season, primarily by Trout Creek and South Fork basins. In 2016, no watershed consistently had the highest maximum EVI, nor did burned or unburned watersheds collectively.

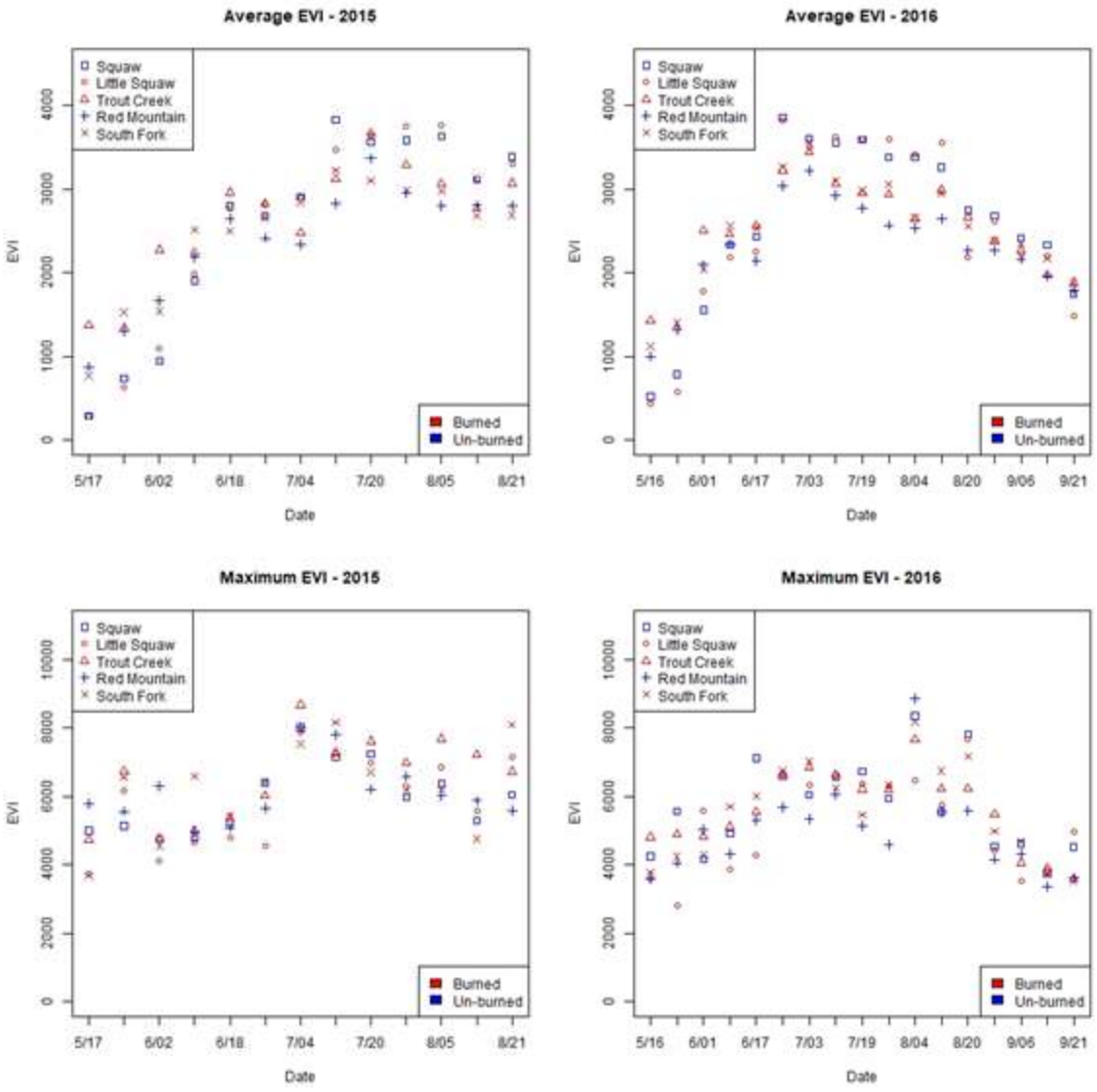

Figure C.1: Average and maximum EVI values for each watershed over each 8-day period in the summers of 2015 and 2016. Blue points indicate unburned watersheds and red points indicate burned watersheds. Annual trends of vegetation greenness indicative of southwest Colorado are apparent in both burned and unburned watersheds. Interestingly, maximum EVI was higher for burned watersheds in almost every 8-day window in 2015, which may be indicative of strong regrowth after the fire in 2013.

APPENDIX D

ATTEMPTS TO CORRELATE ESTIMATED TOTAL SUSPENDED SOLID CONCENTRATIONS TO TIME VARIANT AND INVARIANT VARIABLES

To identify which watershed characteristics are most strongly associated with increased sediment loads, all independent variables identified (Table 2.1) were correlated to estimated average total suspended solids concentration (TSS_{norm}) values over 8-day intervals (Figure D.1).

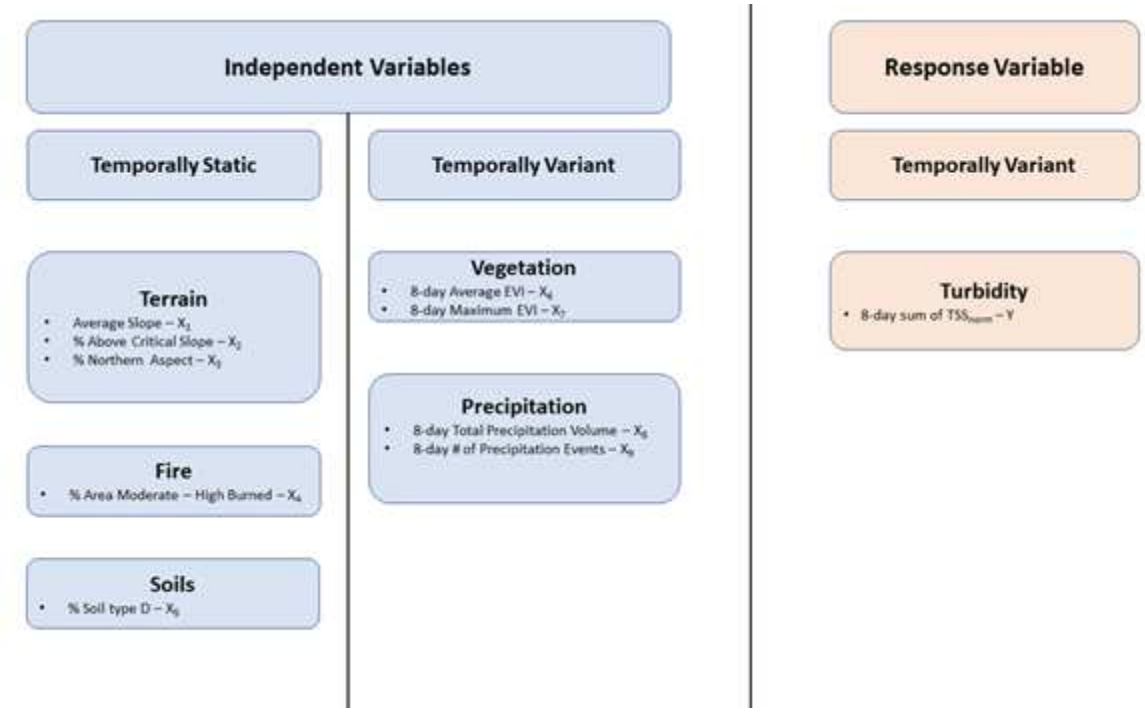

Figure D.1: Variables associated with post-fire sedimentation used for correlation and regression models against the response variable TSS_{norm}, which was calculated using turbidity measurements captured in the field. Each temporally variant variable is quantified for all 8-day windows that turbidity data was available for. Temporally static variables were assumed not to change throughout the study period of 2015 and 2016.

Each temporally static independent variable was correlated individually to the annual sums from the 2015 and 2016 field seasons using Spearman's correlation. These independent variables were held constant for each watershed while TSS_{norm} sums varied. Temporally variant variables, which include average and maximum EVI, precipitation intensity and volume, and TSS_{norm}, were calculated for each EVI-defined 8-day period, which had the lowest temporal resolution at 8-days. These independent

variables were individually correlated to the 8-day sums of TSS_{norm} for all watersheds. Because of the low number of input variables, especially for temporally static dependent variables, correlations were bootstrapped with 1000 repetitions to verify correlation results. Correlation bootstraps were run for burned watersheds, unburned watersheds, and all watersheds combined for each variable. When comparing both burned and unburned watersheds together, few watershed characteristics can be directly correlated to increased TSS_{norm}. When all data are plotted against each other, few visible patterns jump out (Figure D.2).

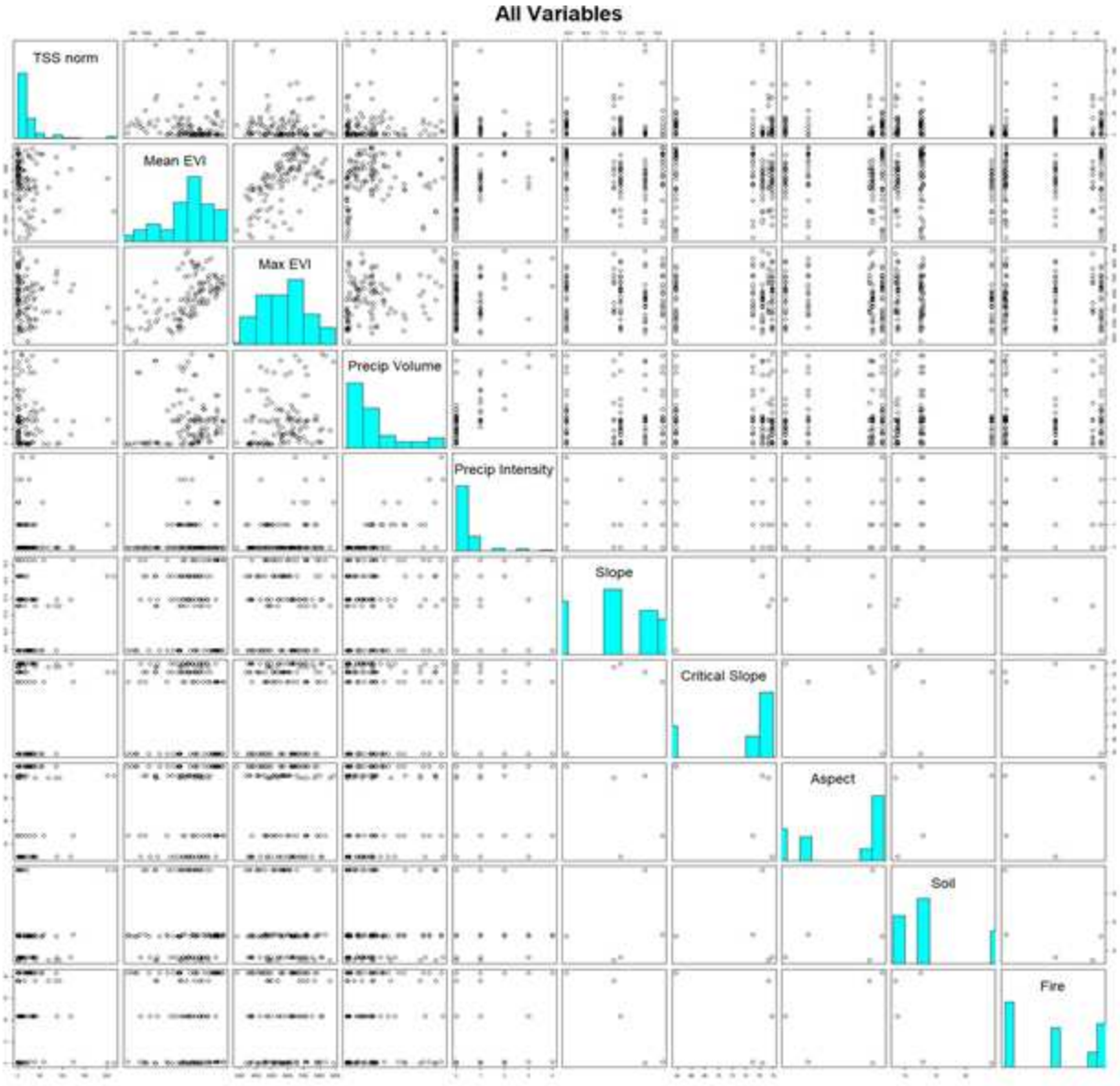

Figure D.2: Plot matrix relating each variable to all other variables. Center diagonal is a histogram of the column/row variable data. Static variables when plotted against temporally variant variables, for example in the upper right region of the plot matrix, create stratified datasets that are difficult to regress across due to the largely overlapping stratified lines.

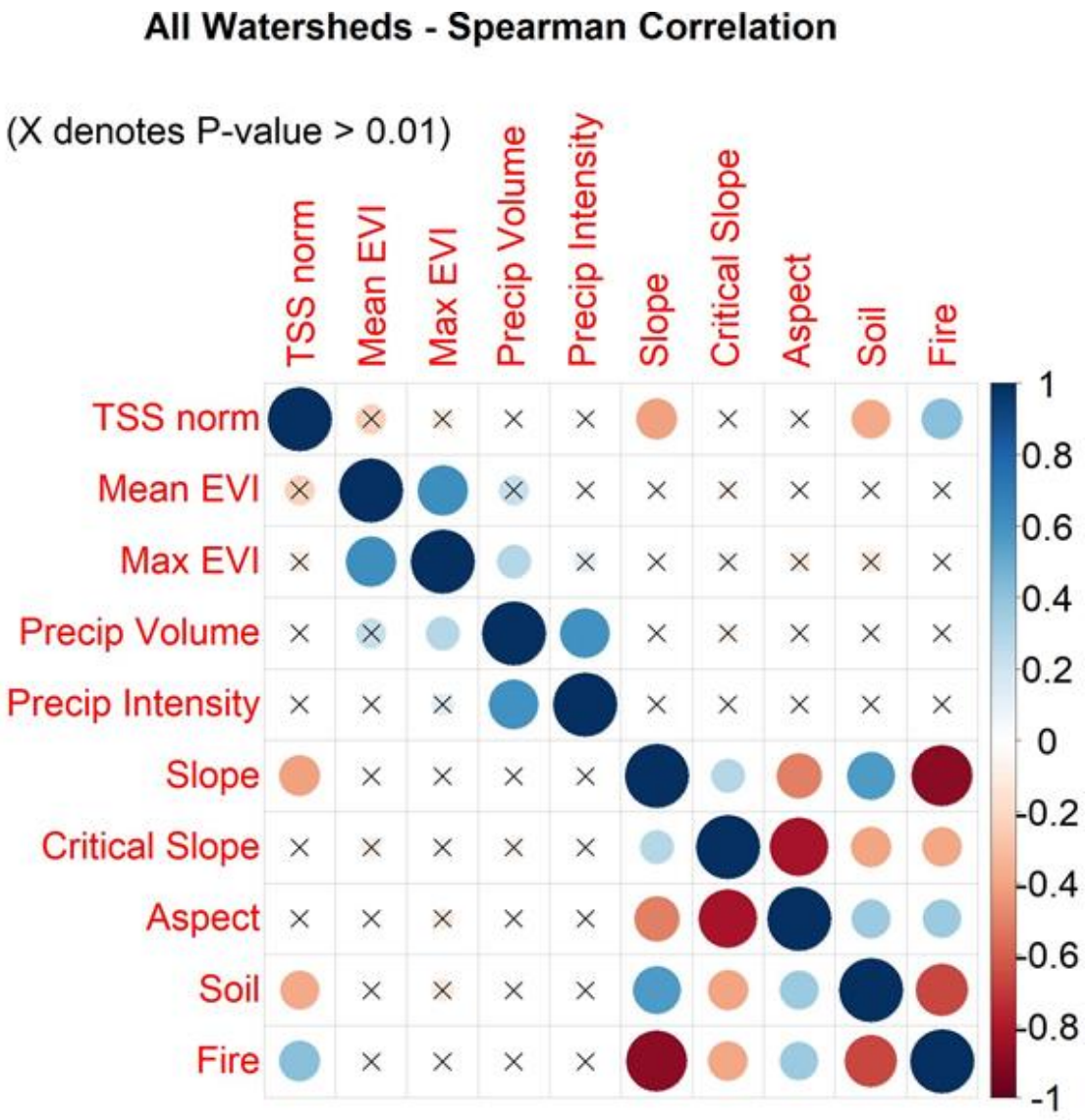

Figure D.3: Spearman's correlation coefficient between all variables from all watersheds in both 2015 and 2016. Denser, more filled in cells indicate a stronger correlation. Blue fill denotes a positive correlation, while red denotes a negative correlation. Insignificant correlations (P-value > 0.01) are denoted by an X. TSS norm denotes the total estimated sedimentation over each 8-day period, normalized for watershed size. Mean EVI and Max EVI denote the mean and maximum EVI value recorded in each watershed over each 8-day period. Precip volume and Precip Intensity denote the total precipitation volume and the total number of high intensity precipitation events recorded in each 8-day period, respectively. Slope represents the average slope of each watershed, Critical Slope denotes the percentage of each watershed above 33 degrees, Aspect denotes the percentage of each watershed with a northern aspect, Soil denotes the percentage of each watershed with a hydrologic soil type rating D, and Fire denotes the percentage of each watershed burned at a moderate to high severity level.

The watershed characteristics with the strongest correlation to increased TSS_{norm} are percent of watershed burned at moderate to high severity, percent of watershed dominated by soil type D, and average slope (Figure D.3). Interestingly, soil type and slope are both negatively correlated to TSS_{norm}, despite being quantified for each watershed by characteristics associated with increased sedimentation, including more erosive soils and steeper slopes.

APPENDIX E

ATTEMPTS TO BUILD SINGLE- AND MULTIVARIATE RESGRESSION MODELS

To identify the extent to which watershed characteristics control sedimentation in both burned and unburned watersheds, a single variable linear regression was run using the built in *lm* linear model function in R, holding normalized Total Suspended Solids (TSS) as the response variable against each independent variable individually. Temporally static watershed characteristics, including average slope, percent of the watershed above 33-degrees, percent of the watershed with northern aspect, soil type, and burn severity were run against annual sums of average total suspended solids concentration (TSS_{norm}), while temporally variant watershed characteristics, including precipitation and maximum and average EVI were run against each 8-day sum of TSS_{norm}. These single variable linear regressions, conducted for burned and unburned watersheds separately, were also bootstrapped, and the mean regression slope and intercept from the bootstrapped model results were used to compare the relative impact of each watershed characteristic on TSS_{norm} loads.

In addition to single variable regressions between each independent variable and the response variable (TSS_{norm}), a multivariate linear regression was run using the same built-in *lm* function in R. TSS_{norm} remained the response variable, while each of the independent variables were input for each 8-day window. This multivariate linear regression was run using all independent variables (Figure E.1), as well as a smaller subset of independent variables selected for stronger correlations with TSS_{norm}.

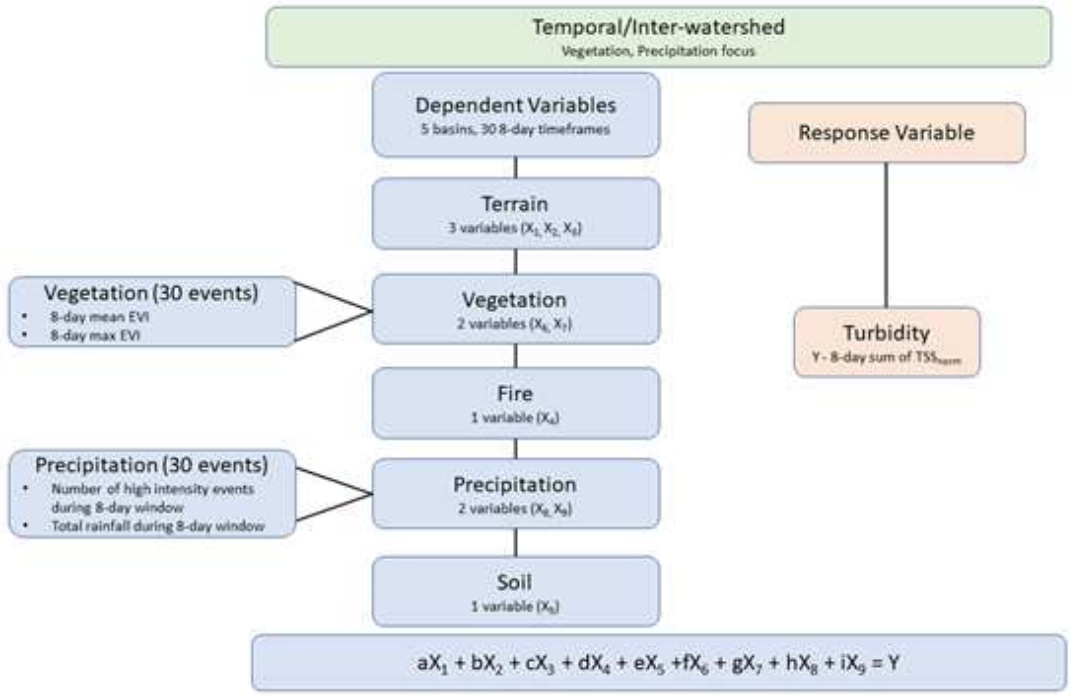

Figure E.1: Multivariate linear regression setup for all variables. Letter coefficients, e.g. k, l, m, represent the calculated coefficient for each variable from the multivariate regression. X_n denotes a vector containing each variable's quantified value for each 8-day period for each watershed in both 2015 and 2016. Y denotes the vector of TSS_{norm} for each 8-day period in each watershed in both 2015 and 2016. X_1 – average slope of each watershed. X_2 – percent of watershed above critical slope. X_3 – percent of watershed with Northern aspect. X_4 – percent of watershed burned at a moderate to high severity. X_5 – percent of watershed dominated by soil type D. X_6 – 8-day average EVI. X_7 – 8-day maximum EVI. X_8 – 8-day total precipitation volume. X_9 – number of high intensity precipitation events in each 8-day window. All X_n and Y vectors are the same length, with a value for each 8-day period that TSS_{norm} was able to be calculated for each watershed.

No statistically significant relation was found between the estimated TSS_{norm} and any individual watershed characteristic using single variable linear regression models. This indicates that no single watershed characteristic is able to fully describe the variance in TSS_{norm} between watersheds and throughout 2015 and 2016 in burned, unburned, or combined groupings. Even watershed characteristics that were significantly correlated with TSS_{norm} (Figure D.3) were unable to describe TSS_{norm} with a linear model (Figure E.2).

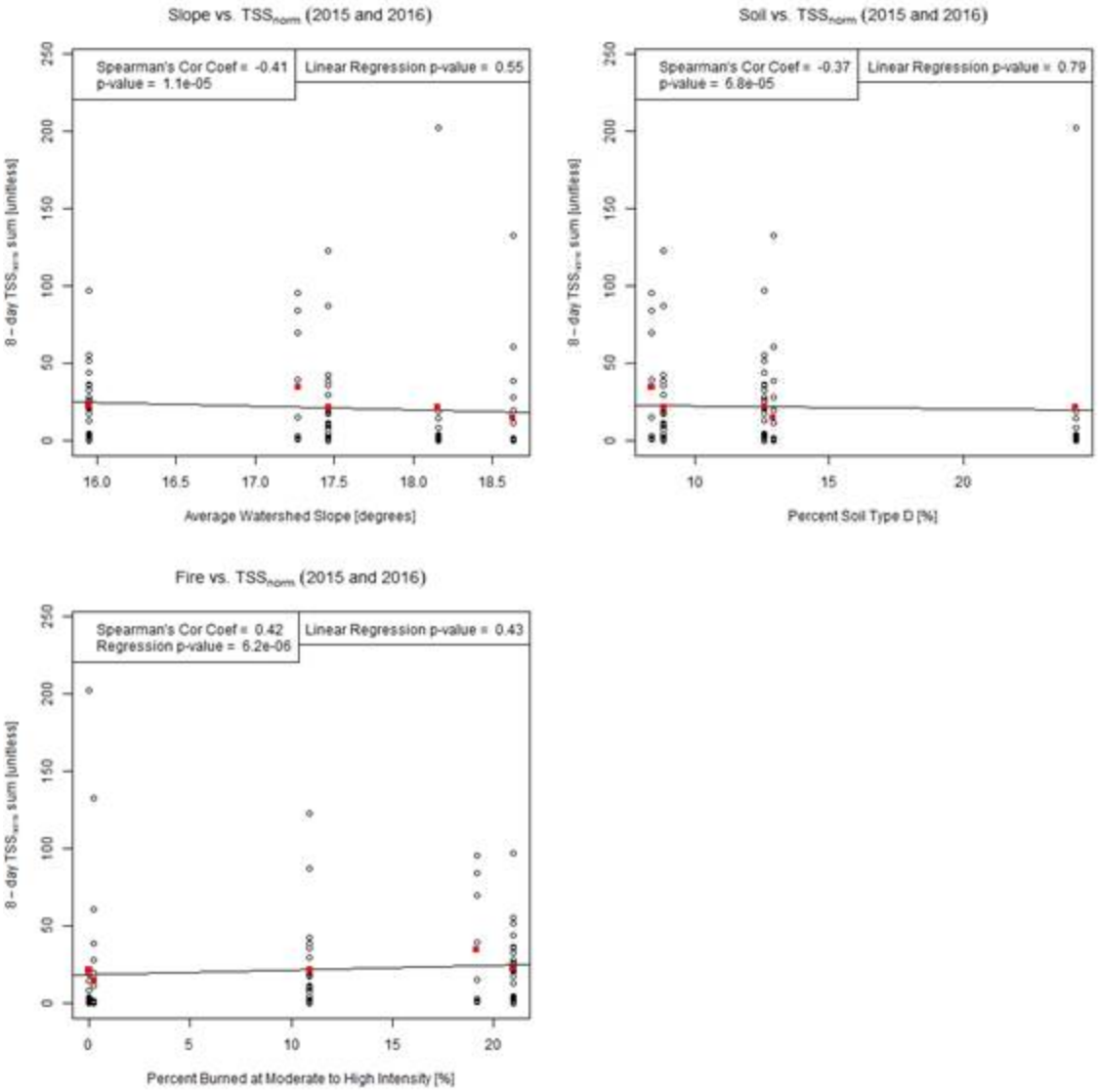

Figure E.2: Attempted linear regression models on watershed characteristics with the strongest correlation to TSS_{norm} – average slope, percent of watershed dominated by type D soils, and percent of watershed burned at a moderate to high severity. Due to static nature of these watershed characteristics, data are stratified into five groupings. Red points indicate the mean 8-day TSS_{norm} value for each watershed. No regression results were statistically significant, despite significant correlations.

To avoid reading too much into data with relatively few points, single variable linear regressions were bootstrapped with 1000 runs. No single variable regression was able to significantly fit the TSS_{norm} data, indicating that no one variable is solely responsible for variations in TSS_{norm} (Table E.1).

Table E.1: Single variable linear regression results for each parameter against the response variable TSS_{norm} after bootstrapping the regression with 1000 runs. No single variable regression was able to significantly explain variations in TSS_{norm}. As expected, the three parameters most closely correlated with TSS_{norm} (slope, soil, and fire) had the highest R^2 values, although these are still far from significant.

Parameter	Regression Slope	Regression Intercept	R^2
Mean EVI	-0.01	36.36	0.03
Max EVI	0	30.88	0.02
Precipitation Volume	-1.99	21.81	0.01
Precipitation Intensity	1.34	18.73	0.02
Slope	-48.77	1133.44	0.39
Critical Slope	-0.08	268.78	0.27
Aspect	8.13	-179.15	0.2
Soil	-2.97	492.7	0.2
Fire	6.87	203.02	0.38

Because no single independent variable was able to describe trends in TSS_{norm} throughout the study period, multivariate regression models were also run including all independent variables (Figure E.1) against TSS_{norm} in both burned and unburned

watersheds. The multivariate regression using all watershed characteristics was unable to describe variations in the response variable TSS_{norm} (R^2 = 0.27). However, three variables in the regression showed statistically significantly significant estimated regression coefficients (p-value < 0.05): the percent of the watershed above 33-degrees (p-value = 7.8 e-4), the percent of the watershed with northern aspect (p-value = 2.3 e-8), and the percent of the watershed with soil types A or B (p-value = 3.0 e-5; Table E.2).

Table E.2: Multivariate linear regression results for all watershed characteristics against the response variable TSS_{norm} in both burned and unburned watersheds.

Watershed Characteristic	Estimated Coefficient	Std. Error	p-value
Intercept	-3541.0	722.7	2.64E-06
Mean EVI	0.0	0.0	7.49E-01
Max EVI	0.0	0.0	6.83E-02
Storm Volume	-2.8	2.9	3.45E-01
Storm Peak Intensity	8.4	9.0	3.53E-01
Average Slope	28.7	33.5	3.93E-01
% Above 33-degrees	15.8	4.6	7.82E-04
% Northern Aspect	41.0	6.9	2.28E-08
% Soil type A-B	-17.2	4.0	3.00E-05

To explore the role of those watershed characteristics played in influencing turbidity following the WFC fires, another multivariate regression was run using only those three characteristics between the four burned watersheds. This regression attempt was also unsuccessful in describing variations in the response variable TSS_{norm} (R^2 = 0.001). None of the three watershed characteristics showed statistically significant estimated regression coefficient values (Table E.3), indicating that the relationship between TSS_{norm} and the studied watershed characteristics is either non-linear or involves more variables not included in this study.

Table E.3: Multivariate linear regression results for selected watershed characteristics against the response variable TSS_{norm} in burned watersheds.

Watershed Characteristic	Estimated Coefficient	Std. Error	p-value
% Northern Aspect	192.95	133.78	0.15
% Above 33-degrees	-0.54	0.37	0.15
% Soil Type A-D	0.52	0.45	0.25